Abstract

The effect of Densification of wood on the performance of wood/graphene/epoxy was studied in this work White teak, also known as Gamari was densified and grounded and incorporated with GNP 0-0.3% to make the composite samples DW. Tests were carried out on this samples to evaluate the mechanical, thermal, electrical and moisture absorption properties. Densification significantly improved filler matrix bonding and load transfer resulting in higher tensile, flexural and impact properties compared to normal wood (WG) composites. Optimum performance occurred at 0.2 wt% GNP where graphene bridging enhanced and increased impact toughness and conductivity without agglomeration. Thermal analysis (TGA/DSC) showed us that higher decomposition initial temperature and residual mass for DW composites confirming improved thermal stability. Despite slightly higher moisture uptake, DW composites showed lower diffusivity due to reduced porosity. Overall this combining of densified wood flour with graphene nano particles gives us composite material with very high strength and good thermal properties and electrical properties for use in structural applications and thermal and electrical insulation applications.

Summary

The main idea of this study is basically to make a stronger and more eco-friendly material by mixing wood, graphene, and epoxy resin together. The goal and objective is to improve the performance of normal composites that have usually use in things like furniture, construction, and even in some automotive parts.

In this research we used a process called densification. Here the wood was treated and pressed so hard it became much harder and less porous than the before state. After that, the densified wood was ground into a fine powder. Then this powder was mixed with a small amount of graphene. Graphene is a super strong carbon material that also conducts electricity really very well and epoxy resin, which was perfectly acted kind of like glue or binder for everything.

We tried different types of sets of mixing ratios to see which one works the best. The sample made with densified wood and about 0.2% graphene gave the best results. This particular composite showed a higher strength, better heat and more thermal stability, and also improved electrical conductivity with compared to the regular wood composites that we tested alongside.

Even though the densified wood tended to absorb a touch moisture its packed structure curtailed water passage. All told the research shows that fusing densified wood, with graphene yields a material that manages to be both eco-friendly and top-tier in performance. Such hybrids could end up in anything, from ultra-light frameworks and insulating boards to gadgets providing an alternative to the usual synthetic fare

Table of Contents

List of Figures:

List of Tables:

Chapter 1: Introduction

Bio based fillers and wood derivatives are receiving growing attention as sustainable, low cost reinforcements for polymer composites because they reduce plastic content and valorize agricultural and wood wastes [1]. Wood flour is a low cost and widely available lignocellulosic filler consisting of cellulose, hemicellulose and lignin that has been incorporated into polymer matrices to reduce material cost and improve stiffness. When it is incorporated into polymer matrices it offers an ecofriendly route to replace petroleum derived polymers reducing both cost and environmental footprint and improves stiffness and dimensional stability [2]. Such wood/polymer composites have found applications in automotive panels, building materials, furniture, packaging, and consumer products where moderate mechanical strength and good processability are needed [3]. However, wood flour based composites often suffer from poor filler matrix adhesion and moisture sensitivity that can limit strength and durability. These issues can lead to weak filler matrix bonding, microvoid formation and premature failure, limiting their use in structural or high performance applications unless suitable surface modification or coupling strategies (e.g., silane, alkaline, or acetylation treatments) are employed [4].

Densification of wood through chemical treatment (alkaline treatment) and mechanical compression (hot pressing) is an established process to produce higher density wood with improved strength and stiffness [5], [6].

In the nanoscale regime, graphene derived materials like nanoparticles, among of them, prove to be reinforcements for epoxy [7]. Adding only just a modest amount can boost stiffness, strength and thermal stability but the payoff hinges, on achieving dispersion and strong interfacial bonding [8]. Blending of the graphene with the nanofillers emerges as a route marrying the bulk virtues of

lignocellulosic substrates, with the potent reinforcement that is offered by nanoscale graphene[9] The resulting hybrids unlocks a synergy by enhancing strength, electrical conductivity and thermal stability, thereby widening of their horizon to components, electromagnetic shielding and lightweight structural panels [10], [11].

Getting wood flour and graphene to disperse with an epoxy matrix is a huge headache largely because their polarities and surface energies don't line up. If the graphene sheets clump, if the filler ends up unevenly scattered or if voids form, during the time of the curing of the composite's mechanical strength can take a hit [12]. Moreover the temperature at which the mixtures is processed and the shear forces applied during mixing and curing shape the epoxy's viscosity and cross-linking behavior, which in the turn influence filler orientation and the quality of bonding [13]. On the side the cost and scalability hurdles of graphene production together with the need to keep densified wood powder consistently high-quality stand out as major obstacles, which is for large-scale manufacturing [13].

In this work we plan to close those gaps of experiments by pitting wood-flour/epoxy/graphene composites against their densified wood-flour counterparts by keeping the processing route and test regime identical. Samples were prepared with three graphene concentrations 0.1 wt % 0.2 wt % and 0.3 wt %. Then subjected to a battery of thermal, electrical and morphological examinations. The overarching question is whether compressing the wood flour improves its affinity, for the matrix and, if graphene and the densified wood operate merely in parallel or interact synergistically to boost performance. By understanding these interactions, this research aims to guide the design of the next generation of bio based hybrid composites that are mechanically strong, thermally stable and environmentally sustainable, also offering renewable alternatives for semi structural and functional material applications.

1.1. Objective of the Study

The objectives of this study are:

- To develop and compare epoxy based composites reinforced with normal and densified white teak wood flour combined with varying graphene nanoparticle contents.

- To investigate how wood densification and graphene addition influence the mechanical, thermal, electrical and moisture diffusion properties of the composites.

- To identify the optimum formulation and understand the synergistic mechanisms that lead to enhanced strength, stability and sustainability in hybrid bio based composites.

Chapter 2: Literature Review

2.1. Introduction

Recent literature shows tremendous work being done to pave the way for development of sustainable polymer composites. Components such as bio fillers, nanofillers and matrix have been researched on thoroughly to understand how their unique characteristics blend together to achieve desired properties. Multitude of work have been done on Wood flour as the bio filler, epoxy as the matrix and graphene as the nanoparticle of choice and using various mechanical and chemical treatments, mode of manufacturing and composition have been explored to optimize the composite materials for better mechanical, thermal and chemical properties. Limitations such as weak fiber matrix adhesion, agglomeration, low quality dispersion among others are roadblocks along the way and this research works to address these issues to improve the overall properties.

2.2. Wood Flour (White Teak)

Wood flour is a fine lignocellulosic powder obtained by grinding and sieving wood residues into micro sized particles which is typically below 500 μm. It is widely used as a renewable and biodegradable reinforcement in polymer composites. The composition of wood flour primarily includes cellulose, hemicellulose and lignin. Cellulose is responsible for strength and rigidity, hemicellulose contributes to flexibility and lignin provides structural stability and hydrophobicity. The ratio of these constituents depends on the species and treatment of the wood. In this project, white teak (Gmelina arborea) wood flour is used due to its light weight, moderate density (400–550 kg/m^3) and uniform grain structure [14]. White teak has a naturally high cellulose content and

good dimensional stability which makes it suitable for use as a reinforcing filler in polymer matrices. Its availability as a by product from furniture and carpentry industries also makes it an economically viable and sustainable material choice [15].

When converted into fine flour, white teak provides a large surface area for interaction with polymer matrices. The mechanical and thermal properties of the resulting composite depend heavily on this interfacial adhesion. However, untreated wood flour can exhibit weak bonding with non polar polymers such as epoxy, polyethylene or polypropylene because the hydrophilic nature of cellulose is incompatible with the hydrophobic polymer matrix [16]. By bathing the material in a solution lignin and hemicellulose are leached away laying bare the cellulose microfibrils and leaving the surface textured enough to boost interlock. Hence white teak wood flour shows a promise, as a filler especially when further refined either chemically or mechanically to sharp its interfacial adhesion with polymer resins [17].

2.2.1. Wood Flour in Composites

The use of the wood flour, in the polymer matrices is attracting the growing attention as part of the push toward bio-based, materials. As a micro-reinforcement wood flour stiffens the composite reduces to be shrinkage and helps lower costs [18]It also boosts biodegradability while cutting the reliance on petroleum-derived plastics. In composites particularly wood-plastic composites (WPCs), wood flour are widely employed in polypropylene, polyethylene and polyvinyl chloride matrices, for the decking, cladding and an automotive interior components. In thermosetting systems like epoxy or polyester resins, the filler acts more as a stiffness enhancer and micro crack arrester [19].

Proper dispersion and wetting are essential to avoid all the voids and stress concentration points. Fine particle sizes and uniform distribution contribute to improve dimensional stability and surface finish. However, excessive wood content increases viscosity and makes the processing difficult. Therefore an optimized filler proportion which is usually around 10–40 wt% for micro size wood flour is adopted to balance mechanical performance and workability [19], [20].

Wood-flour-reinforced composites is specially appealing for consumer grade applications where modest mechanical strength and a pleasing aesthetic suffice. They appear in dashboards, door panels, furniture boards and a host of building components. Their ecological edge comes from the ability to incorporate fillers while still providing adequate thermal and mechanical stability [21]. Nonetheless drawbacks such, as moisture sensitivity, dimensional instability and weak interfacial bonding persists spurring research into formulations and surface-treatment approaches.

2.2.2. Utilization of Waste Wood

Turning the wood wastes into something has been risen to an environmental and economical goal, in today's materials engineering. The woodworking and furniture sector churns outs quantities of sawdust, shavings and offcuts most of which ends up as low value biomass. Grinding that waste into wood flour opens a route to add value and keep the material in a loop. When waste wood flour is woven into polymer composites it not eases the burden, on landfills. Also trim the composite's overall carbon footprint [17].

A series of investigations have demonstrated that treated wood waste flour can substitute a portion of polymer without compromising functional performance. Employing the post-consumer or industrial wood residues aligns neatly with sustainable development objectives curbing

deforestation and preserving resources. Moreover chemical pretreatment of this waste raises cellulose purity, which in turn enhances bonding efficiency with the polymers. White teak dust has been used successfully as a filler in hybrid composites with natural fibers such as abaca or pineapple showing notable improvements in tensile and flexural strength [22]. Therefore, the valorization of wasted wood flour not only mitigates waste management challenges but also contribute to the creation of low cost, high performance green composites.

2.3. Graphene

Graphene is a two dimensional allotrope of carbon consisting of a single layer of sp^2-bonded carbon atoms arranged in a hexagonal lattice. It represents one of the strongest and most conductive materials ever discovered. Since its isolation in 2004, graphene and its derivatives including graphene oxide (GO), reduced graphene oxide (rGO) and graphene nanoplatelets (GNPs) have found extensive application in polymer nanocomposites [23]. Even at very low concentrations this graphene can dramatically improve the mechanical, electrical and thermal performance of a host polymer because of its exceptional intrinsic properties.

The incorporation of graphene into polymer composites aims to exploit its high aspect ratio, large surface area and superior interfacial interactions with polymer chains [24]. These features allow graphene sheets to act as load bearing bridges and barriers to heat and moisture diffusion. Yet achieving a dispersion of graphene within a matrix remain a stubborn hurdle as the material's pronounced van der Waals forces readily drives it toward an agglomeration [25]. Consequently researchers habitually lean on a toolbox that includes ultrasonication, shear mixing, solvent blending and surface functionalization to coax over the sheets into an spread. The prospect of pairing graphene with fillers such, as wood flour is especially compelling because it fuses

nanoscale reinforcement with bulk bio-based particles yielding the composites that exhibit a hierarchical reinforcement architecture [26].

2.3.1. Structure of Graphene Nanoparticles

Graphene nanoplatelets (GNPs) consist of a graphene sheets stacked atop one another typically giving a thickness of about 3–10 nm and dimensions ranging, from 1 to 10 μm [26] Each platelet still displays the honeycomb lattice of carbon atoms, where every carbon form three σ-bonds and retains a π-electron that to underpins its conductivity. The sp^2 hybridization bestows graphene with its geometry and its high electron mobility [24]. When graphene is partially oxidized the introduced oxygen containing groups create sites that can bond with matrices such, as epoxy.

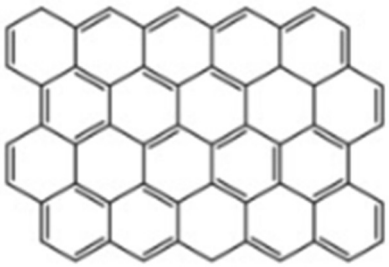

Figure 1: Structure of Graphene [27]

The specific surface area of GNPs can reach 30–60 m^2/g allowing efficient stress transfer in between the matrix and filler [28]. The high aspect ratio that enables the formation of percolation networks at very low loadings (0.1–0.5 wt%) resulting in drastic and very large improvements in conductivity and stiffness. However to maintaining exfoliation and preventing restacking during mixing are crucial to retain these advantages [29]. Because of its architecture, graphene forces gases and moisture to wind a path, around its platelets acting as an effective diffusion barrier. This

trait becomes especially useful when graphene is blended with wood flour, in epoxy formulations, where it helps to curb the moisture-sensitivity of fillers.

2.3.2. Properties of Graphene

Graphene's intrinsic qualities are truly extraordinary which is why it stands out as a top-tier nano reinforcement. Its Young's modulus breaks the 1 TPa barrier its tensile strength can soar to 130 GPa and its thermal conductivity can top 5 000 $W \cdot m^{-1} \cdot K^{-1}$ [30] Moreover it boasts a specific surface area and an electrical conductivity, in the realm of 10^6 $S \cdot m^{-1}$. These impressive numbers of the trace back, to a delocalized π-electron network that lets electrons move freely across the plane [24]. Beyond of the electrical perks graphene also enjoys a chemical stability resisting corrosion, oxidation and even very high temperatures.

In polymer composites the inclusion of the graphene can simultaneously improve an suite of characteristics. On the side the material imparts added stiffness and strength by enabling load transfer. Thermally graphene speeds up this heat dissipation. Slows the degradation while its electrical nature supplies antistatic and shielding functions [31] Its two-dimensional geometry also encourages crack deflection, bridging and energy absorption during fracture, which together boosts toughness. Still these advantages depend heavily on how the graphene's dispersed and how well it interact with the surrounding of polymer chains [32].

2.3.3. Application of Graphene in Composites

Incorporating graphene, into polymer composites has dramatically reshaped nanomaterials research. Even a modest loading typically between 0.1 wt% and 1 wt% can yield pronounced performance gains [29]. Within epoxy matrices the graphene functions as reinforcing phase that spans microcracks stiffens the material. Boosts its stability. Its sheet like geometry creates

pathways, for electrons endowing insulating polymers with electrical conductivity. Recent investigations have unveiled the epoxy composites imbued with graphene exhibit tensile, flexural and impact strength relative, to the neat epoxy. When graphene is present, in amounts it functions as a stress-bearing bridge, however at loadings the sheets tend to aggregate spawning imperfections that serve as stress concentrators.

Therefore an optimum loading usually is around 0.2 wt% is found to deliver the best mechanical balance. Thermal analysis of such composites often reveals delayed degradation and higher residual mass confirming improved thermal stability [33]. In hybrid systems of that combine graphene with natural fillers such as wood flour or cellulose fibers synergistic effects are observed. Graphene improves the stiffness and conductivity while the lignocellulosic filler enhances the load transfers and toughness [34]. Such multiscale reinforcements are being explored for lightweight automotive components, electromagnetic shielding materials and bio based structural composites [24].

2.4. Epoxy Resin

Epoxy resins are thermosetting polymers characterized by the presence of reactive epoxide groups that crosslink with hardeners such as amines, anhydrides or polyamides. They are known for their high mechanical strength, dimensional stability, strong adhesion and chemical resistance [35]. Epoxy resins form the matrix phase in a wide range of fiber reinforced composites and coatings. Their three dimensional network structure arises from curing reactions that transform the liquid resin into a rigid solid with excellent mechanical and dielectric properties [35].

In composite materials epoxy acts as the load transfer medium between the reinforcement and the external stress. Its compatibility with both organic and inorganic fillers makes it a versatile matrix for developing hybrid materials. Epoxy resins can also be modified to adjust viscosity curing speed and flexibility according to the processing requirements. For example the Lapox Metapalm system used in this study provides low viscosity (800–1200 mPa·s) and moderate curing temperature which facilitate proper dispersion of fillers and elimination of air voids[36]. Epoxy resins are also thermally stable up to about 150 °C and has an good adhesion to wood and graphene surfaces making them an ideal choice for this project [37].

2.4.1 Properties of Epoxy Resin

Resin's standout traits arise from its cross-linked molecular network. Once the cure is complete the material shows a modulus robust compressive strength and precise dimensional stability. Its density hovers around the 1.1–1.2 g / cm^3 while the tensile strength typically falls, in between 40 and 90 MPa depending on the formulation[38]. The glass-transition temperature (Tg) generally spans over 70 °C to 150 °C delivering stability under moderate conditions [39]. Furthermore the low shrinkage during the curing minimizes the internal stresses and cracking [38].

Epoxy is also an excellent electrical insulator although when combined with conductive fillers like graphene it can form semi conductive or antistatic composites [37]. The barrier properties of epoxy against moisture and chemicals are well established although extended exposure to water can cause some plasticization and reduction in stiffness. Its relatively low viscosity before curing allows uniform mixing of micro and nano fillers leading to homogeneous composites. Thus, epoxy provides an ideal platform for studying the combined effects of densified wood and graphene reinforcements.

2.4.2. Application of Epoxy Resin in Composites

Epoxy resins are extensively used in structural, electrical and protective composite applications. They serve as matrices in glass fiber, carbon fiber and natural fiber reinforced laminates [37]. In recent years epoxy has become a preferred matrix for nano reinforced composites due to its ability to form strong covalent and hydrogen bonds with nanoparticles [40]. The addition of graphene or silica nanoparticles can enhance mechanical and thermal stability without significantly increasing weight [33], [39].

When combined with wood flour epoxy can produce sustainable composites with high stiffness and moderate strength suitable for building panels, furniture components and automotive parts. The hydroxyl groups dangling from cellulose readily engage the epoxide groups of epoxy forging an bond [41] Yet raw wood often soaks up the resin in a way spawning voids. Simple pretreatments like alkaline washing, densification and the like tune the surface chemistry encouraging resin uptake and slashing defect of formation. Consequently epoxy/wood-flour/graphene blends emerge as a class of composites striking a balance, between high strength, toughness and environmental sustainability.

2.5. Densification of Wood

Densification is a treatment that raises wood's density, and strength and dimensional stability. It begins by stripping away lignin and hemicellulose a step known as delignification follows with hot pressing, under precisely controlled temperature and pressure. This sequence collapses all the network re-orients of the cellulose microfibrils and encourages hydrogen bonding among them.

As a result the densified wood displays stiffness, lower porosity and an smoother surface, than untreated wood [6].

The concept of densification has gained renewed interest because it transforms low density wood species into high performance materials that can rival-metals or synthetic composites. Delignified and compressed wood could achieve tensile strengths above 500 MPa [42]. The combination of chemical and thermal treatments leads to a uniform microstructure with minimized defects and improved load bearing capacity. For composite fabrication, densified wood can be ground into fine powder (densified wood flour) that retains these microstructural advantages. Such powders exhibit higher rigidity, better compatibility with polymers and lower water diffusivity making them valuable as fillers in hybrid bio composites [6].

2.6. Conclusion

The literature review suggests that incorporating Densification of wood in the methodology might improve the mechanical, thermal and electrical properties of the developed nanocomposites. The densified fiber will improve the surface morphology and adhesion while graphene will improve the load transfer and conductivity. A few questions arise regarding the prospect of this work:

- To what extent does densification of wood impact the overall properties?
- Will densification of wood improve against natural degradation components like moisture?
- What would be the optimum graphene loading for maximum performance?
- Will the newly developed nanocomposite maintain stability under high thermal inertia?

Chapter 3: Materials and Methods

3.1. Introduction

The materials, manufacturing techniques and testing procedures in this section were employed to fabricate the desired specimens and analyze their properties. White teak wood flour was grounded and used as the desired microfiber due to its strong fiber structure, epoxy resin as the desired polymer matrix due to the extensive work done using this matrix in previous literature, GNP as the preferred nanofiller due to its ability to improve mechanical properties and conductivity. Densification of wood was carried out through preliminary delignification and hot pressing at high pressure and temperature. The samples were fabricated following established ASTM standards and tests were carried out to analyze the mechanical, morphological, electrical and thermal properties of the developed composite materials.

3.2. Material

3.2.1. Wood:

White teak wood was chosen for its lightweight properties, strong fiber structure, sustainability, and moderate density (400–550 kg/m³). Wood particles of 50 mesh (297 microns) were used as filler material, as teak dust acts as a micro-filler, improving composite homogeneity [43], [44].

Figure 2: Raw white teak

3.2.2. Epoxy and Hardener:

As a thermosetting polymer, epoxy resin has good and well studied interfacial adhesion with wood flour and nanoparticles. The stable mechanical properties of epoxy resin make it preferable for studying filler effects such as those of Densified wood flour filler [45], [46].

Figure 3: Epoxy and hardener

Lapox Metapalm System B was chosen as the preferred epoxy resin for its low viscosity of 800-1200 mPas and a low density of 1.15 g/cm^3 while the counterpart hardener has 0.97 g/cm^3 density and 300-600 mPas viscosity. It has good adhesion properties and is thermally stable and well resistant to water and chemical attacks. The property table is shown below:

Table 1: Properties of Epoxy Resin

Property	Unit	Reference	Resin Value	Hardener Value	Mix Value
Viscosity at 25 °C	mPa·s	ASTM D2196	800–1200	300–600	500–800
Density	g/cc	ASTM D792	1.00–1.20	0.95–1.00	–
Mixing ratio (resin: hardener)	w/w	–	–	–	100:50
Pot life	Minutes	ASTM D2471	–	–	20–35
Peak exotherm temperature	°C	ASTM D2471	–	–	Max 75
Surface dry time	Hours	ASTM D5895	–	–	150–180
Touch dry time	Hours	ASTM D5895	–	–	230–260

3.2.3. Graphene Nano Particles:

XFQ021 GNP were sourced from XFNANO, China and were of 99.5% purity. The properties of the Graphene Nano Particles:

Table 2: Properties of GNP

GNP Material Property	Value
Electrical Conductivity	800–1100 S/cm
Apparent Density	0.09–0.13 g/cm³
Tap Density	0.13–0.16 g/cm³
Lateral Size	5–10 µm
Surface Area per Gram	31.2 m²/g
Usage	Fillers

3.3. Densification

The samples were heated in an oven at 100°C for an hour. The oven's vent was kept open to let the steam escape (since moisture moves from high pressure to low pressure). After drying, the samples were sealed quickly in a zipper bag to prevent reabsorption of moisture from the environment.

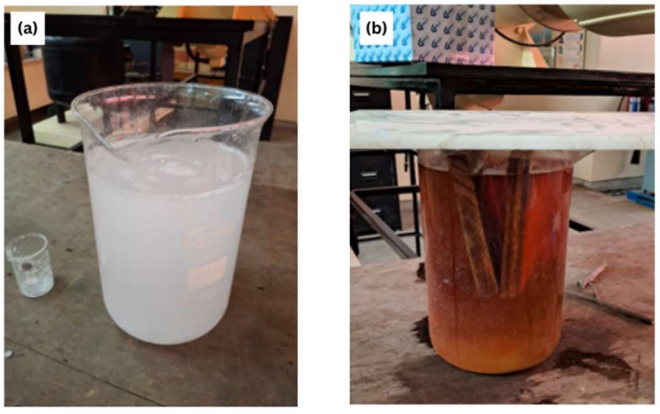

Figure 4: (a) Alkaline solution, **(b)** Brown solution indicating delignification

An aqueous 2.5M NaOH and 0.4M Na_2SO_4 solution was prepared, and dried wood samples were submerged in it for 24 hours [6]. The reaction turned the solution brown and generated heat, confirming lignin and hemicellulose extraction. After 24 hours, the darkened solution indicated completion, and the wood samples were removed for next treatment [47].

Figure 5: Hot-pressing under 2 MPa pressure at 165°C temperature

The delignified wood samples were subjected to hot pressing under a pressure of 2 MPa at 165°C for 30 minutes. The thickness of the sample decreased by 40% from initial thickness of 20mm to 12mm.

3.4. Fabrication of Specimen

3.4.1 Wood Flour Preparation

Using a wood planer machine, the skin of densified wood was removed. The wood skins were then blended for 15 minutes to convert them into powder form. To achieve the desired particle size, the wood flour was sieved through a 50-mesh (297 μm) sieve using a sieving machine.

Figure 6: 50 mesh sized wood flour

3.4.2 GNP mixing and dispersion

The GNP was first dried in an oven for removing moisture at 100^0 for 30 minutes and then mixed with acetone in a magnetic stirrer for 1 hour at 2000 rpm with a 0.2% w/v GNP content. Shear mixing was carried out for 30 minutes for better dispersion. The component A part of the epoxy resin was then added to the graphene acetone solution maintaining a varying ratio of 0.1%, 0.2%,

0.3% GNP w/v in a magnetic stirrer and stirred while heating for 1 hour to evaporate the acetone in the mixture. The remaining acetone was completely evaporated and the air trapped inside the mixture was then evacuated by heating for an hour in a vacuum oven at 80^0 C [48].

Figure 7: GNP dispersion using magnetic stirrer

3.4.3 Casting and Curing

The sample molds were designed using SolidWorks software according to the ASTM International standards. The dimensions were maintained strictly to the following test methods: ASTM D638 for tensile specimens, ASTM D790 for flexural specimens, ASTM D4812 for impact specimens, and ASTM D5229 for moisture absorption specimens [49], [50] [51][52]. Following the design phase, the molds were fabricated using additive manufacturing (3D printing) technology.

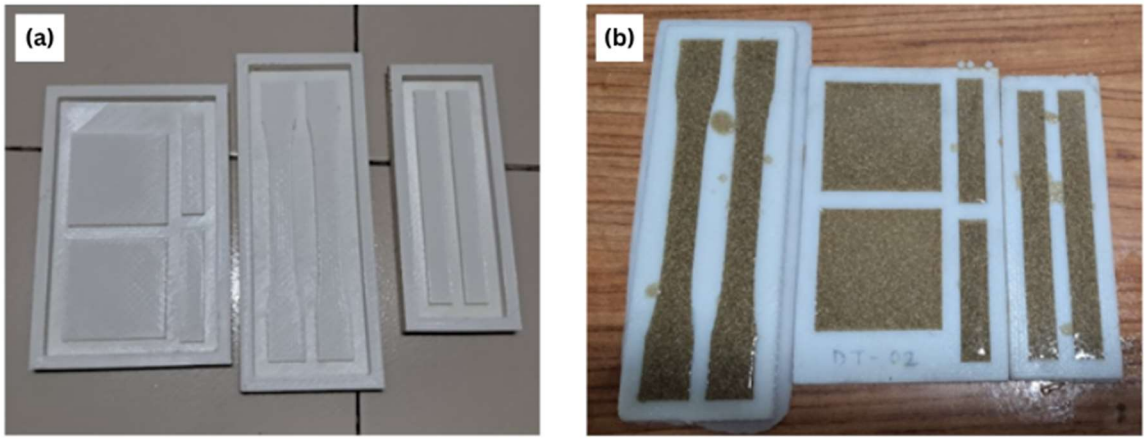

Figure 8: (a) Mold preparation, **(b)** sample preparation

A mixture of silicone and hardener (50:1 ratio by weight) was blended and poured into the 3D-printed mold, where it was left for 5 hours to dry. This process created a flexible mold which is suitable for casting the final composite samples. The wood-graphene-epoxy mixture, prepared at the specific predetermined ratios, was then poured into the silicone mold and allowed to dry for 24 hours. After complete cure process, the final sample was carefully demolded.

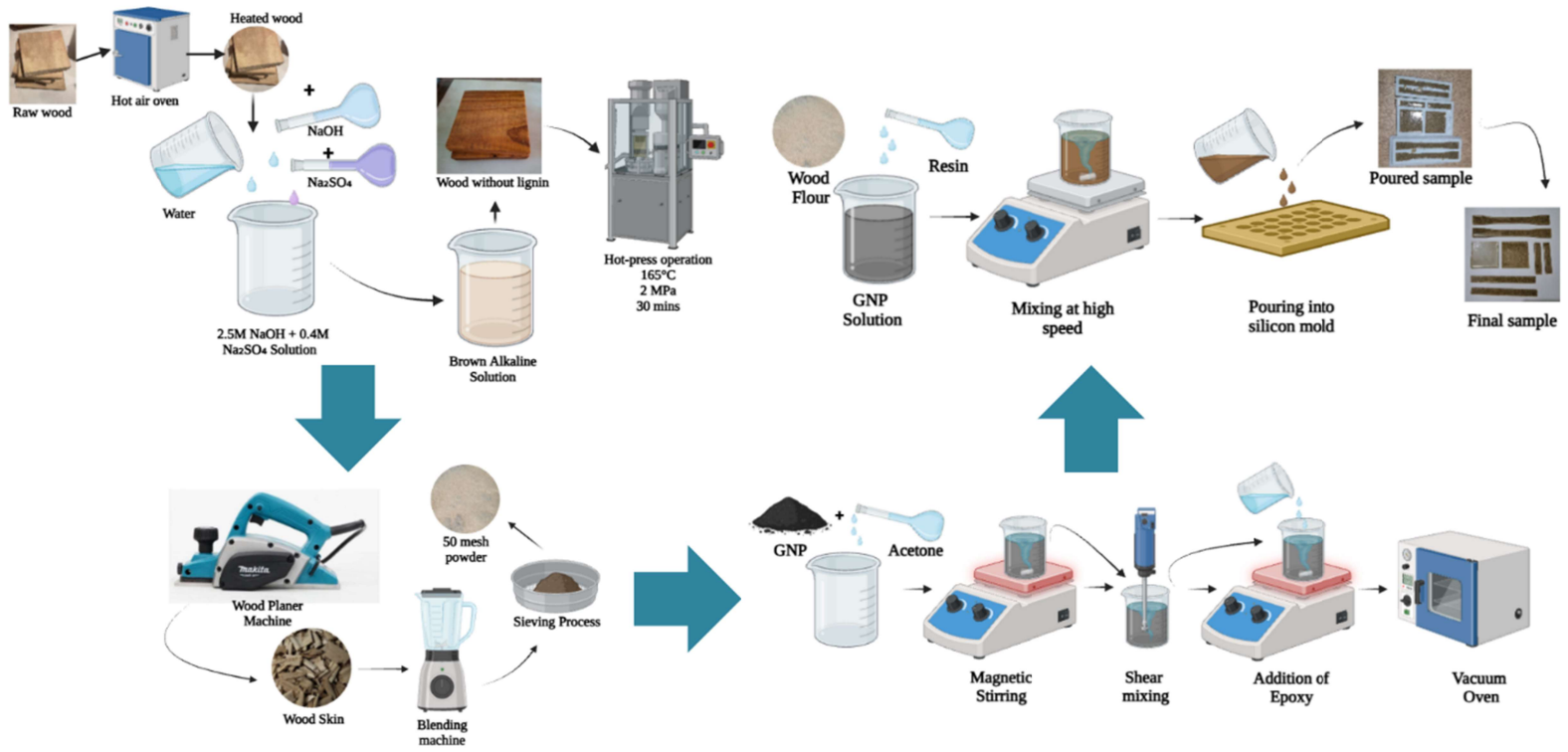

Figure 9: Schematic diagram of sample preparation

3.5. Characterization

3.5.1. Morphological properties

SEM snapshots were taken at an array of magnification each peeling back a layer of the composite's world. At magnification the images sketch the fracture silhouette the spatial choreography of filler particles and the continuity of the epoxy matrix. By crank up the magnification shifts the focus, to the nanoscale ballet of graphene nanoplatelets the glue-like bond that ties the epoxy to the wood-derived fillers whether their densified form and the microscopic drama of failure from the crack whisper, to its relentless propagation and the eventual pull-out of material. A careful eye was kept on how the graphene spread through the epoxy because when the sheets bunch together or form of clusters the mechanical response of the composite tends to shift [12]. In densified wood flour composites, special focus was placed on the matrix infiltration into the compacted cell wall regions and the extent of filler matrix interlocking while for normal wood flour composites observations were made on porous zones, weak interface regions and void induced crack paths [6].

These SEM observations provided crucial insights into the microstructural integrity enabling correlation between the microstructural features and the mechanical properties of the graphene reinforced wood epoxy composites.

3.5.2. Thermal Properties

TGA and DSC were used to study the thermal properties and understand the thermal stability of the samples. ASTM E1131 was followed to carry out TGA [53]. 3-10 milligrams of grounded

samples were heated slowly at a rate of 20 ◦C/min upto 600 ◦C. TGA curves help understand the thermal stability in terms of the material decomposition rate against temperature.

DSC was carried out following the ASTM D3418-15 standard [54]. A similar heating rate of 20 ◦C/min was applied from room temperature upto 600 ◦C. Plots were produced plotting total heat conducted per unit time against temperature to give a portrayal of the heat flow through our samples.

3.5.3. Tensile properties

Tensile tests were carried out at the specimen fabricated following the ASTM 638- type I standard for plastic composites [49].

Figure 10: Tensile test setup

The tests were carried out at 2 mm/min. A Stress strain graph was plotted and the Young's Modulus was calculated using Equation

$$E = \frac{\Delta\sigma}{\Delta\epsilon} \quad (1)$$

Where, Δσ represents the difference in stress values between two specific data points within the linear segment of the stress-strain curve.

Similarly, Δ∈ denotes the difference in strain values corresponding to those stress data points, measured within the absolute strain range of 0.001 to 0.003.

The specific modulus of elasticity was measured using

$$E_{smT} = \frac{E}{\rho} \tag{2}$$

Where E_{smT} is the Specific Modulus of Elasticity and ρ is the density of the material.

3.5.4. Flexural properties

Three-point bending tests were conducted using a Shimadzu universal testing machine (UTM). The Prepared specimens' dimension was 127 × 12.7 mm in length and width, with a uniform thickness of 3.2 mm. The support span was maintained at 52 mm according to the ASTM standard of D790, maintaining the required span-to-thickness ratio of 16:1 [52].

Figure 11: Flexural test setup

A crosshead speed of 3 mm/min was applied during testing. From the resulting stress-strain curves, flexural modulus of elasticity, and specific modulus of elasticity were calculated.

To determine flexural modulus of elasticity,

$$E_f = \frac{\Delta\sigma}{\Delta\varepsilon} \tag{3}$$

Here, E_f is the flexural modulus of elasticity

$\Delta\sigma$ is the difference of stress values in two data points in the linear region of the stress strain curve

$\Delta\varepsilon$ is the difference of the strain values in two data points corresponding the stress points

To determine the specific modulus of elasticity,

$$E_{smF} = \frac{E_f}{\rho} \tag{4}$$

Here, E_{smF} is the Specific Modulus of Elasticity in MPa.cm^3/g

E_f is the Flexural Modulus of Elasticity in MPa

ρ is the density of the material in g.cm^{-3}

3.5.5. Impact properties

Unnotched Cantilever Beam Impact strength test of samples was conducted following ASTM D4812 standard [51] . The average width and thickness of the samples were 6.2mm and 3.2mm. From the test we have got the impact energy values in joules from which we have measured the impact strength values from the following equation,

$$E_I = \frac{E}{b \times h} \times 10^3 \quad (5)$$

Here,

E_I = Impact Strength (in Kj/ m^2)

E= Impact Energy (in J)

b = Width of sample (in mm)

h = Thickness of sample (in mm)

3.5.6. Diffusivity properties

The diffusivity constant (Dz) is an important parameter in the moisture absorption test. This test was performed following the ASTM D-5229 standard [50]. Square-shaped samples with dimensions of 55 mm × 55 mm were first air-dried to remove all initial moisture content. The dried samples were then immersed in water under laboratory conditions for a period of one month until moisture equilibrium was achieved. The mass of each sample was recorded every 24 hours. Before weighing, the samples were gently wiped with a dry cloth to remove any surface water and ensure accurate measurements.

The change in mass was calculated using the following equation,

$$\%change\ in\ mass = \left|\frac{W_i - W_b}{W_b}\right| \times 100 \quad (6)$$

Here,

W_b = The oven dried mass of the specimen in grams

W_i = The mass of the specimen in i^{th} day in grams

To calculate the diffusivity constant (Dz), the following equation was used,

$$D_z = \pi\left(\frac{h}{4M_m}\right)^2\left(\frac{M_2 - M_1}{\sqrt{t_2} - \sqrt{t_1}}\right)^2 \quad (7)$$

H = thickness of the samples

M_m = Moisture Equilibrium

$\left(\frac{M_2 - M_1}{\sqrt{t_2} - \sqrt{t_1}}\right)$ is the slope of the two linear parts of the graph

3.5.7. Electrical Conductivity

A high resistance meter was required to perform electrical conductivity measurement on insulating or semi-conductive materials as reported in the literature [55].

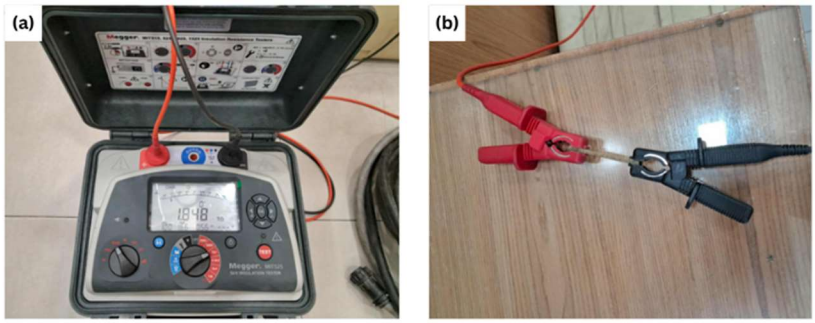

Figure 12: (a) resistance meter, **(b)** sample setup for conductivity test

This test was conducted to analyze the effect of graphene percentage on electrical conductivity of densified wood samples compared to the normal wood samples. In this study, specimens containing 0%, 0.1%, 0.2% and 0.3% graphene in normal and densified wood with dimensions of 50 mm × 12.4 mm were tested using a Megger MIT 525 Insulation Resistance Tester (Megger Group Limited, Dover, United Kingdom). The procedure was done following the guidelines of ASTM D257 [56].

To calculate the conductivity the following equation was used:

$$\mho = \frac{L}{R \times b \times h} \tag{8}$$

Here,

$\mho$ is the conductivity of the material in Simens/meter

L is the active length of the specimen where the probes were connected

R is the insulation resistance in ohms

b is the thickness of the specimen

h is the width of the specimen

3.5.8. Design of Experiments

For systematically evaluate the influence of the densification and graphene content on composite performance, nine different sets of sample groups were prepared. The design of experiments is summarized in Table 4 by detailing the matrix type, filler form and graphene nanoparticle concentration used in each formulation.

Table 3: Design of Experiments

Sample	Descriptive name	Matrix	Wood Filler Type	GNP %
E0	Epoxy (neat)	Epoxy	—	—
WG0	Wood (normal) +Graphene	Epoxy	Normal Wood Flour	0%
WG1	Wood (normal) +Graphene	Epoxy	Normal Wood Flour	0.1%
WG2	Wood (normal) +Graphene	Epoxy	Normal Wood Flour	0.2%
WG3	Wood (normal) +Graphene	Epoxy	Normal Wood Flour	0.3%
DW0	Densified wood +Graphene	Epoxy	Densified Wood Flour	0%
DW1	Densified wood +Graphene	Epoxy	Densified Wood Flour	0.1%
DW2	Densified wood +Graphene	Epoxy	Densified Wood Flour	0.2%
DW3	Densified wood +Graphene	Epoxy	Densified Wood Flour	0.3%

3.6. Conclusion

The materials, method of fabrication and testing and characterization processes followed an already established framework of developing new type of composite materials. The availability of

the materials, controlled densification and manufacturing methods with external parameters included, standardized test methods as mentioned ensures comparability and reproducibility and provides multiple scope to build on this work and further enhance this field of composites in material sciences and technology.

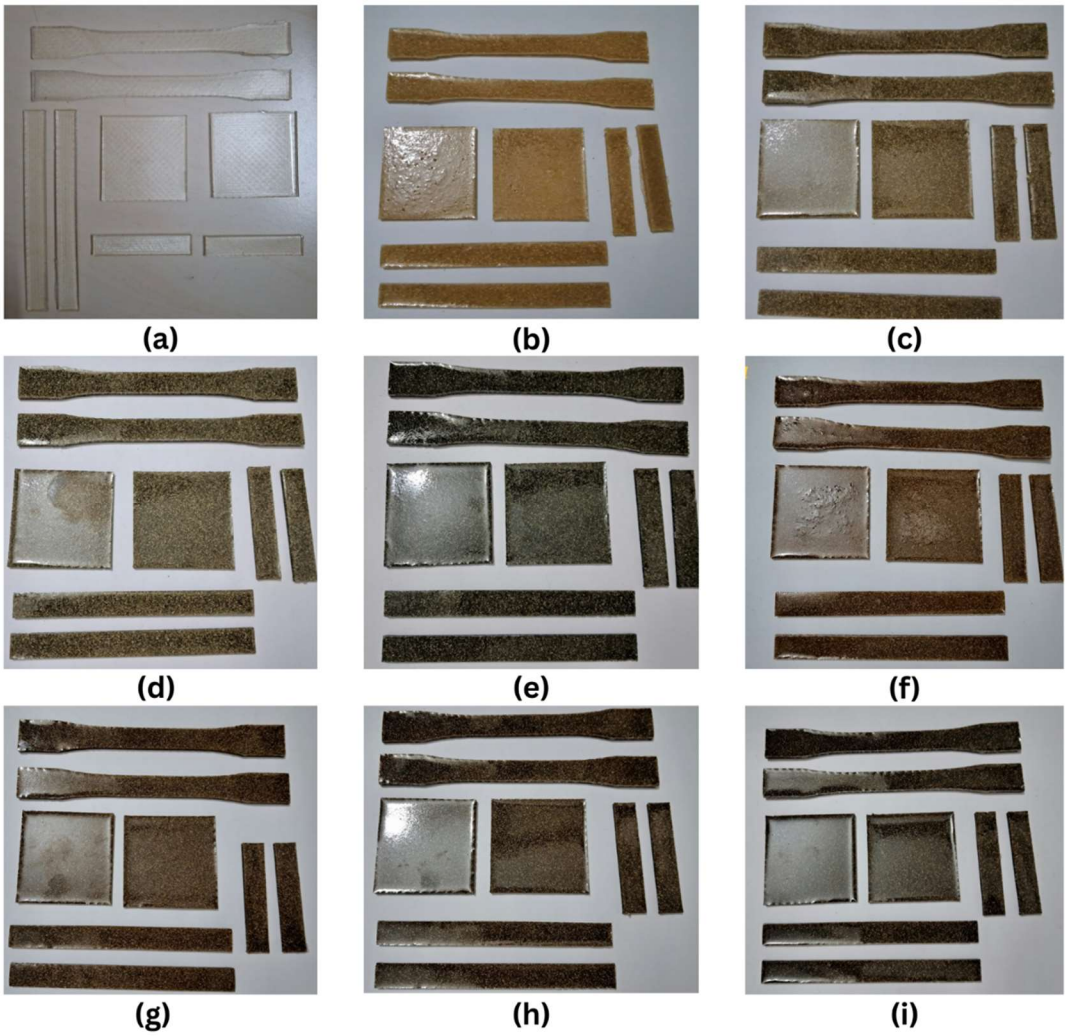

Figure 13: (a) Neat epoxy samples, **(b)** WG0 samples, **(c)** WG1 samples, **(d)** WG2 samples, **(e)** WG3 samples, **(f)** DW0 samples, **(g)** DW1 samples, **(h)** DW2 samples, **(i)** DW3 samples of tensile, flexural, impact and moisture test

Chapter 4: Result and Discussion

The result analysis was done on the test results of the tensile, flexural, impact, moisture and thermal tests. After necessary calculations graphs and bar charts were prepared to make comparison among all nine sets of samples. For result section, the main focus was on the densified wood sample if it increases the strength in these samples.

4.1. Morphological characteristics

The SEM of the WG0 composite reveals a fracture surface that's decidedly uneven and riddled with many pores. A scattering of fiber, pull-out tracks and empty voids points to an adhesion between the untreated wood flour and the epoxy matrix. Air bubbles and interfacial cavities pepper the scene confirming that the resin sadly failed to wet the filler or infiltrate it fully which in turn led to debonding under load. Zones where cracks seem to emanate from around these bubbles suggest that the micro-voids act as stress concentrators, guiding cracks to travel along the filler-matrix boundary, than cutting through the matrix itself. The micrographs show wood fragments whose lumens remain uncrushed a sign that the usual wood framework stayed porous and loosely compacted allowing cracks to snake easily through the fragile cell-wall zones [6].

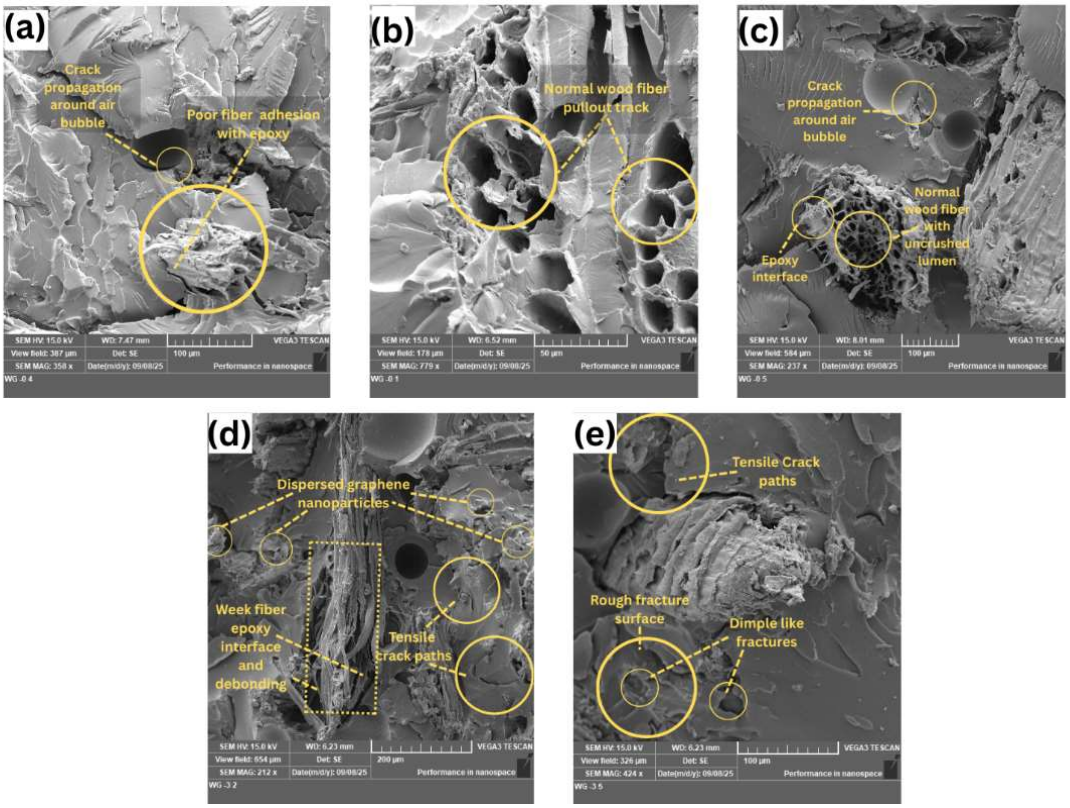

Figure 14: SEM of WG 0 samples **(a)** Fiber epoxy adhesion **(b)** Pullout tracks **(c)** Crack propagation; SEM of WG 3 samples **(d)** Graphene dispersion and crack paths **(e)** Fracture properties

Embedding nanoparticles into wood samples (WG3) provokes clear shifts in in the microstructural landscape. The surface morphology now exhibits fracture pathways, an hallmark of energy dissipation, during failure. While graphene flakes are discernibly scattered throughout the epoxy matrix small agglomerates linger in many spots. These dispersed graphene island, acting as a micron-scale reinforcements curb crack propagation and encourages crack deflection thereby underpinning the tensile and impact performance recorded for this composition. At higher magnification, dimple like fractures and a rough uneven fracture surface can be observed which is characteristic of semi ductile failure. These micro dimples are indicative of plastic deformation and crack blunting in contrast to the smooth brittle morphology of WG0 [57].The tensile crack

paths appear branched and irregular, showing that graphene addition modified the stress distribution and fracture behavior of the epoxy matrix.

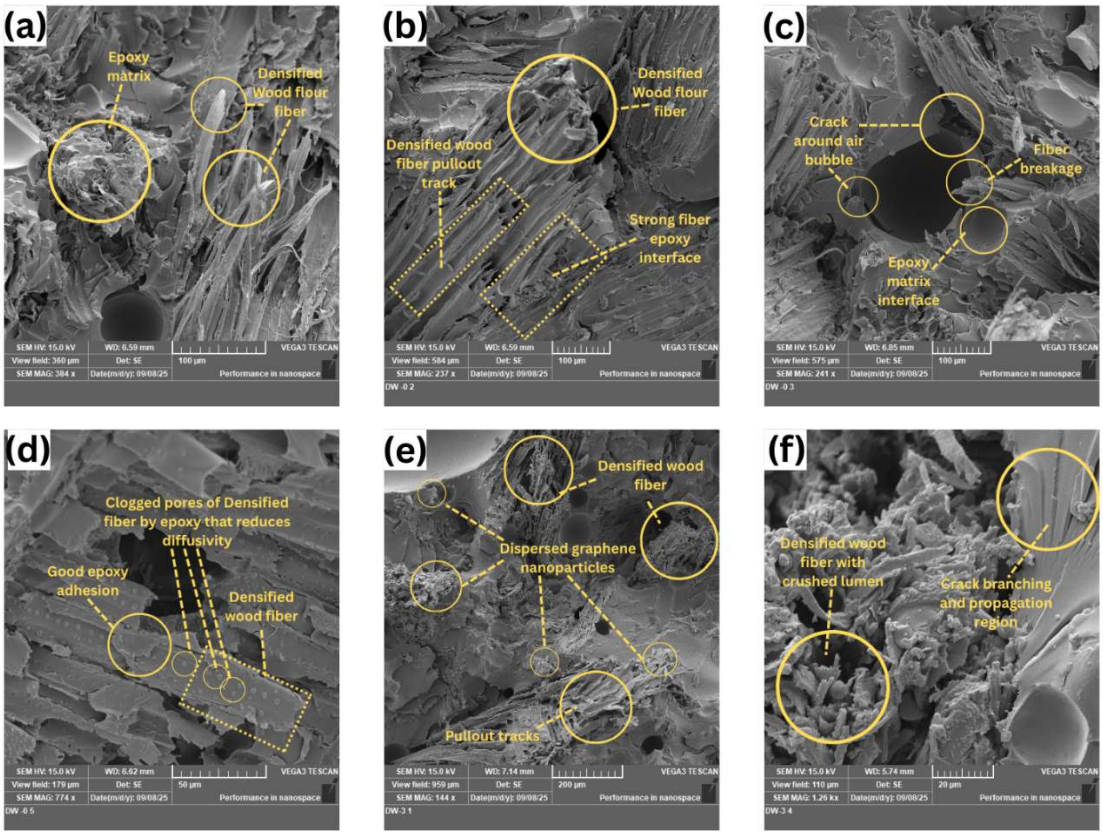

Figure 15: SEM of DW0 samples: **(a)**Densified wood flour morphology**, (b)** Fiber epoxy adhesion, **(c)** Fiber breakage and crack propagation; SEM of DW 3 samples: **(d)** Densified wood flour morphology, **(e)** Graphene dispersion **(f)** Crushed lumen architecture of densified wood fiber

In densified wood samples, the fracture surface shows a compact and well bonded microstructure with densified fibers tightly embedded in the epoxy matrix. Comparing with normal wood flour composites, the fiber pull out and voids are greatly reduced confirming better matrix infiltration and wetting. Some small air bubbles and associated microcracks remained but their propagation is limited by the dense, compressed fiber structure. Epoxy penetration into the clogged pores of the

densified fibers further improves interlocking and reduces diffusivity. The rough fracture texture indicates enhanced load transfer.

With graphene addition, the fracture surface becomes rougher showing dispersed graphene particles embedded in the epoxy phase and bridging between fibers [58].These features contribute to crack deflection, branching and bridging enhancing fracture toughness. The crushed lumens of densified fibers enable deep resin infiltration and strong mechanical anchoring resulting in fewer signs of debonding.

4.2. Tensile Strength

Under static loading (tension, bending, compression) wood-flour/thermoset composites often fail in a brittle manner. When bonding is good, cracks cut through the matrix and particles, causing wood fragments to break rather than simply debonded. SEM fractography confirms this: for example, an epoxy–lignin composite with wood flour showed predominantly broken wood fibers and little pull-out, corresponding to a rough, tortuous fracture surface (enhanced toughness). If the interface is weaker, failure includes larger particle pull-out and voids. Thus the macroscopic fracture process is a mix of matrix cracking, particle rupture and pull-out, depending on local adhesion and stress state.

The Tensile tests showed the dominance of densified wood samples over the normal wood ones in terms of max tensile strength, tensile modulus and strain at break. DW0 had the highest tensile strength at 23.74 Mpa while NW 0 at 20.61 Mpa. An increase of 15%, 34%, 40% and 5% was seen in the max tensile strength for Densified wood samples over normal wood samples at graphene

concentrations of 0%, 0.1%, 0.2% and 0.3% respectively. This suggests that graphene affected the ultimate tensile strength negatively, but the graphene agglomeration effect was much less on the DW samples for tensile properties.

Maximum tensile modulus was seen for DW 2 at 1315 Mpa, more than double of WG 2. Without graphene, DW 0 showed a modulus of 1090 Mpa while WG 0 showed 931.6 Mpa. With graphene addition DW showed an upwards slope while WG showed a downwards one. This supports the belief that Densification strengthens composite materials' tensile properties against agglomeration effects.

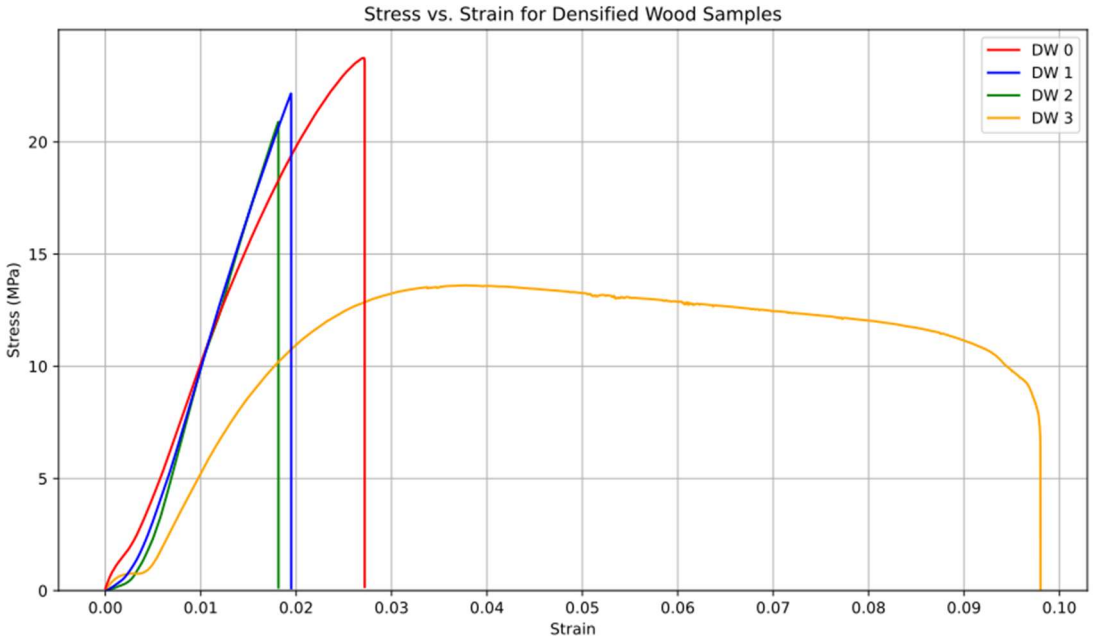

Figure 16: Stress-strain curve of DW samples

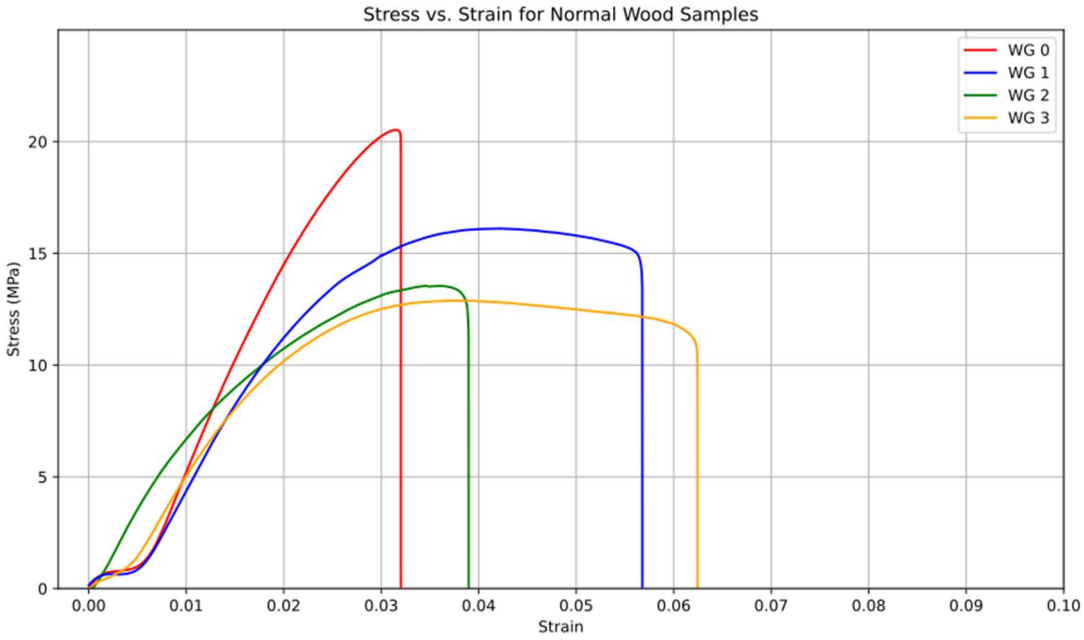

Figure 17: Stress-strain curve of WG samples

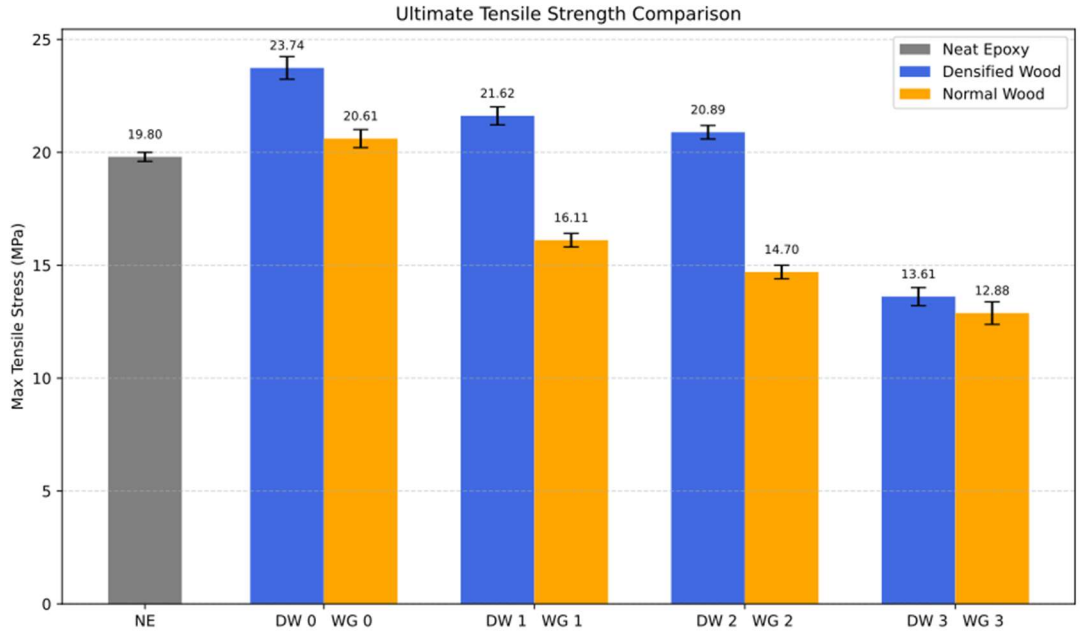

Figure 18: Comparison of ultimate tensile strength among NE, NW, DW samples with varying graphene content (0%, 0.1%, 0.2%, 0.3% wt)

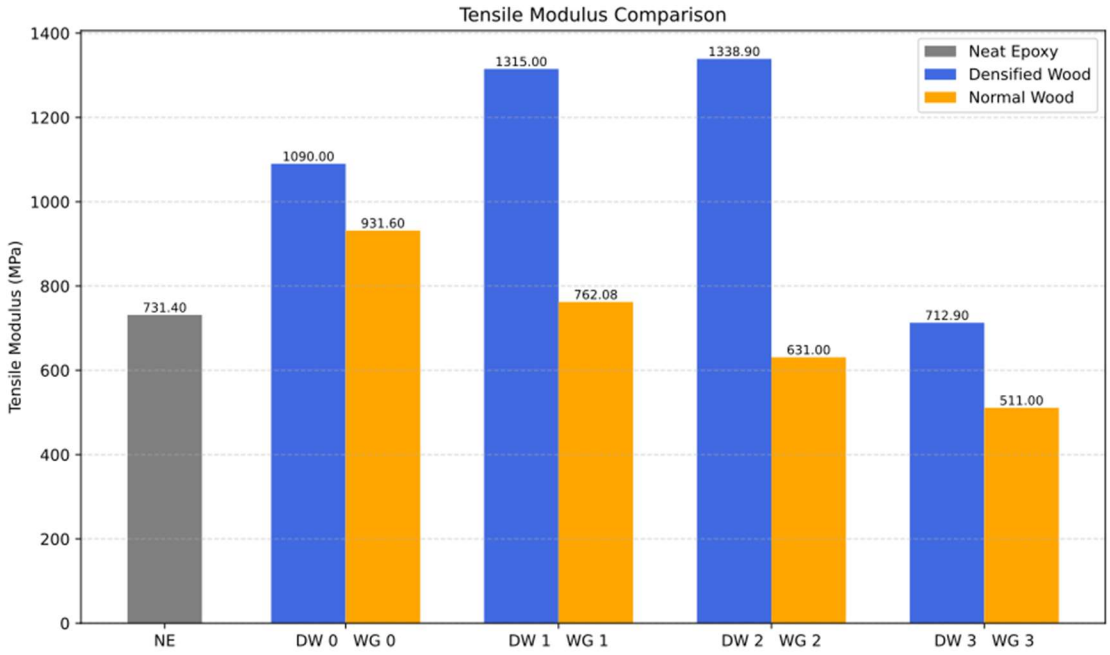

Figure 19: Comparison of tensile modulus among NE, NW, DW samples with varying graphene content (0%, 0.1%, 0.2%, 0.3% wt)

DW samples showed higher ultimate tensile strength and tensile modulus compared to the WG samples mainly because of the Densified wood's microstructure and molecular interactions. The Densified wood flour consists of highly aligned cellulose fibers. The Densification process crushes the wood cells and brings cellulose chains closer. The hydrogen bonding between them is also enhanced resulting in the ability of the DW samples to take larger tensile loads compared to WG ones [59]. The delignification of the wood during the densification helps the tensile properties of the DW samples by enabling better hydrogen bonding with the matrix with the added benefit of the composite having more cellulose-matrix bonding ratio resulting in higher strength [60].

While greater fiber matrix bonding enhanced the DW properties, the higher lignin and hemicellulose content of the WG content resulted in lesser tensile properties. The DW samples have higher number of hydrogen bonds in the Cellulose Microfibrils due to densification. This number of bonds increase further with the addition of Nanoparticles in between the tightly packed cellulose fibers. The Graphene nanoparticles added are similarly rich in carbonyl and hydroxyl groups on its surface while normal wood structure is more porous and lesser surface contact is expected between the cellulose fibers and the graphene nanoparticles in the WG samples compared to the DW samples [61].

4.3. Flexural Strength

In terms of ultimate bending stress, DW 0 shows slight improvements over WG 0 samples. This can be credited to the same factors that played a role in the superiority of the Densified Wood samples over the normal wood ones in tensile properties matrix such as the microstructure which consisted of highly aligned cellulose fibers and enhanced hydrogen bonding [59]. Even with graphene addition at 0.1% concentrations level, DW 1 performed 20% better than the WG 1 samples at 53.38 Mpa and 44.30 Mpa respectively. This can similarly be attributed to the higher surface contact of the densely packed cellulose fiber of the DW 1 samples with the Carbonyl and Hydroxyl groups of the graphene nanoparticles [61].

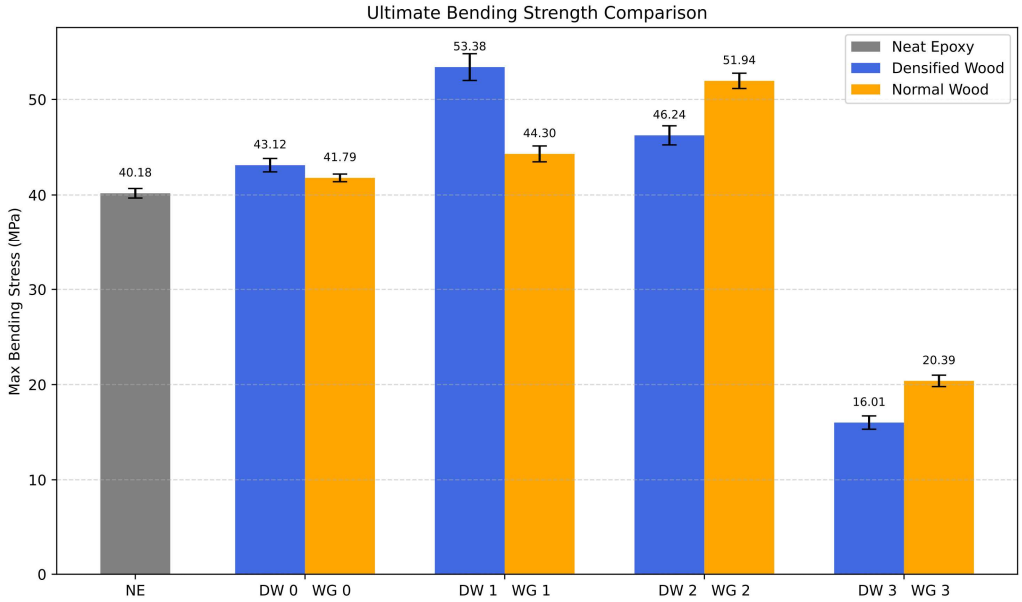

Figure 20: Comparison of ultimate bending strength among NE, NW, DW samples with varying graphene content (0%, 0.1%, 0.2%, 0.3% wt)

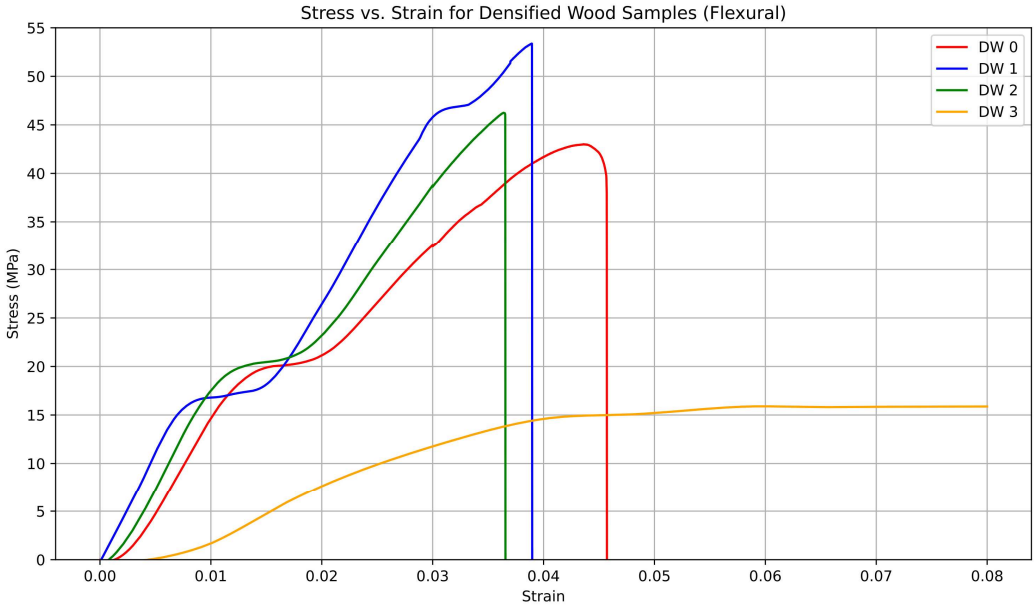

Figure 21: Stress-strain curve for DW samples

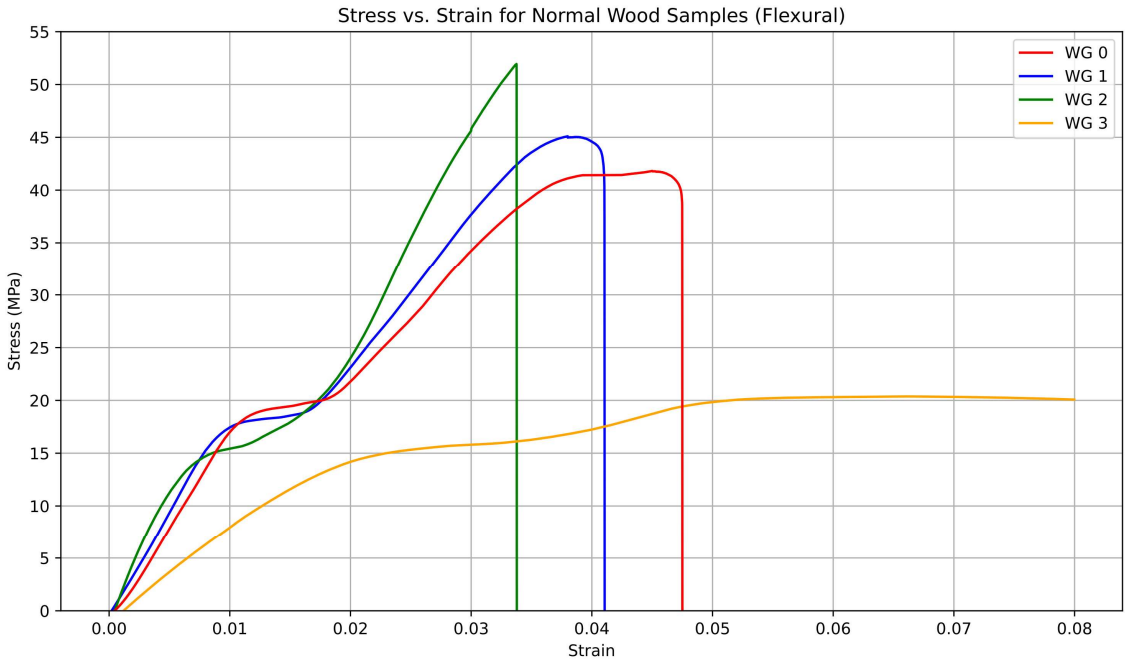

Figure 22: Stress-strain curve for WG samples

However, for further addition of graphene at 0.2% the ultimate bending stress decreases for DW 2 but increases for WG 2. DW 2 and DW 3 show stress of 46.24 Mpa and 16.01 Mpa respectively which are lower than 51.94 Mpa and 20.39 Mpa of WG 2 and WG 3 respectively. While agglomeration and percolation exist together, lesser agglomeration enables the high graphene induced DW samples to have higher tensile properties compared to the WG ones while higher percolation enables the high graphene induced WG samples to have better flexural properties. Instead of surface contact ratio, the percolation threshold of the graphene nanoparticles may play a role here. DW 2 and DW 3 samples have higher density and thus lower porosity due to the mechanical processes performed on the wood samples. The higher porosity of the normal wood samples enables the large pore networks on the fiber surfaces to host larger networks of the graphene nano particles enforcing larger bridges. This bridges predominantly exist in the WG 2

and WG 3 samples more than the DW 2 and DW 3 samples allowing them to show greater flexural stress [62].

4.4. Impact strength

In the case of densified wood, the combined effects of heat, chemical treatment, and applied pressure compress the cellular wall of the wood. This process reduces internal porosity and increases density [6] .For this the woods matrix becomes stiffer and can transmit impact forces more efficiently to the surrounding epoxy–graphene reinforcement network. The compressed surface wall allows better epoxy infiltration which is seen in SEM. Due to stronger wood–epoxy adhesion there is fewer weak spots where cracks could start. As a result more energy is required to break the composite [63]. In densified wood samples, cracks have to pass through a denser and stronger network. This creates more crack deflection and branching, consuming more energy that results in higher impact strength. In normal wood samples cracks can easily propagate through weak porous zones [64].

In this experiment densified wood samples showed better performance in impact strength than normal wood samples.

The addition of graphene nanoplatelets (GNP) influences the behavior of both densified wood (DW) and normal wood (WG) epoxy composites. For densified wood composites, impact strength increased with graphene content up to 0.2 wt% and here the maximum value was observed. This improvement occurred due to the ability of small amounts of well-dispersed graphene to bridge microcracks, deflect crack paths, and transfer stress more efficiently between the epoxy matrix and the wood nano fibers [57].

On the other hand at higher graphene content (0.3 wt%) impact strength decreased. This reduction is related to the agglomerations of graphene particles at higher loadings which act as stress concentrators instead of reinforcements [65]. At a higher graphene content, the epoxy mixture becomes thicker (higher viscosity), which makes it harder to flow into the wood structure. This result in poor penetration near the wood surface and leave small voids or weakly bonded areas. Such defects make crack propagation easier and reduce the overall energy absorption capacity of the composite [66].

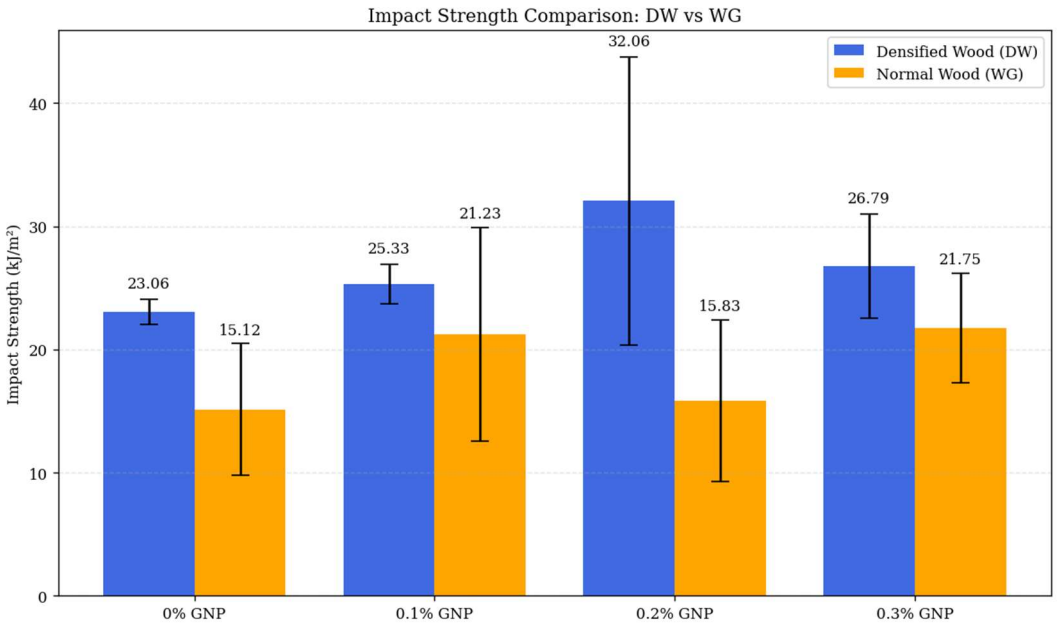

Figure 23: Comparison of impact strength between WG and DW samples with varying graphene content (0%, 0.1%, 0.2%, 0.3% wt)

For the normal wood composites, the effect of graphene addition was less consistent. A moderate improvement was seen at 0.1 wt% GNP, but the impact strength decreased at 0.2 wt% before increasing slightly again at 0.3 wt%. This irregular trend occured due to the higher porosity of

normal wood which makes proper epoxy infiltration more difficult as the resin viscosity increases with graphene addition [66]. As a result, graphene reinforcement in normal wood composites is less effective and the presence of voids or incomplete wetting leads to larger sample-to-sample variability.

Overall, the results suggest that around 0.2 wt% graphene content is the optimum value for the DW composites where the reinforcement effect of graphene is maximized. Beyond this amount agglomeration and impregnation issues of particles dominate and reduces toughness. In comparison, WG composites show less improvements because of their porous structure and weaker matrix infiltration.

4.5. Electrical Properties

Electrical conductivity in composite materials highly depend on the distribution of the conductive filler (i.e. graphene) throughout the structure. Graphene contributes to conductivity creating a continuous conductive path allowing the electrons to flow through the material. At lower concentrations of graphene (<0.1%), the graphene particles are dispersed as isolated fillers and it limits the electron transport. As the graphene content increases (≥0.2%), the inter particle distance decreases and facilitates the formation of interconnected conductive pathways which enhances electrical conductivity [67]. Graphene itself is highly conductive with a natural electrical conductivity of around 10^6 S/m. When it is added to an insulating material like epoxy, it acts like a bridge (nano filler) that helps electrons move because of strong interactions (called π-π interactions) between graphene particles [68].

In this study, the test results show that conductivity increases with the graphene content in both normal and densified wood samples. When 0.1% graphene was added, there was only a slight improvement in conductivity. This suggests that the amount of graphene was not enough to form a proper conductive network which is found in SEM. It was still below the percolation threshold.

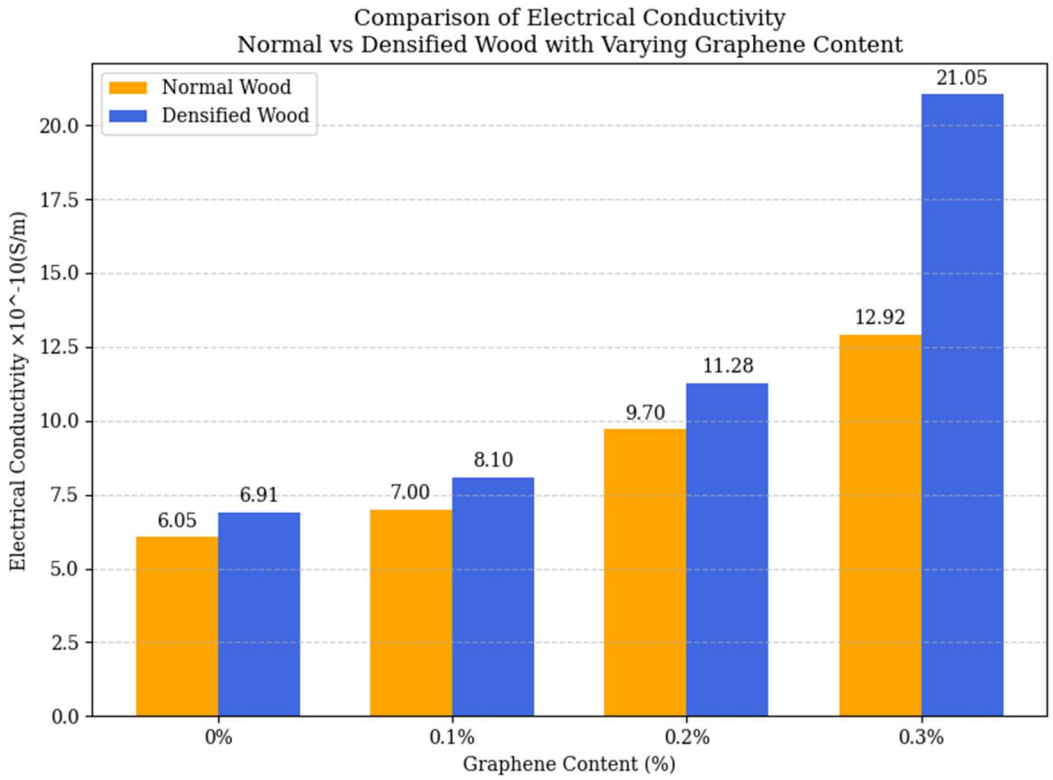

Figure 24: Comparison of electrical conductivity between WG and DW samples with varying graphene content (0%, 0.1%, 0.2%, 0.3% wt)

Furthermore, comparing two types of wood (Normal and densified), the dataset shows that densified wood consistently shows higher conductivity than normal wood at every graphene concentration. Densification compresses the wood's structure slashing its porosity and carving nano-channels between the cellulose nanofibers [69]. This tighter packing aligns the filler particles uniformly and trims resistance, which in turn smooths electron transport. The compacted matrix

curbs electron scattering, allowing charge carriers to glide easily and boosting conductivity. As the cellulose fibers are squeezed together graphene can embed itself firmly within the wood. The altered microstructure eases electron transport compared with wood, whose porous architecture hampers electron migration [70].

Consequently when the graphene loading is kept constant densified wood displays a conductivity, than conventional wood composites. In the series of measurements the densified wood (DW) specimens consistently outperformed the wood in conductivity at every graphene loading level. This advantage stems from the densification step, which compresses the structure into a matrix and thereby smooths the path, for electron transport. As previously noted the addition of graphene gave the conductivity a boost. Of all the samples DW3 emerged as the performer reaching a conductivity of 21.05×10^{-10} S/m.

4.6. Diffusivity Test

When the wood-epoxy-graphene hybrids were dunked in water they followed the diffusion pattern. At the outset moisture content rose almost in lockstep with the root of time tracing a line. As the soak was been continued, the absorption rate eventually flattened out leveling off at once the samples reached their equilibrium moisture content. This behavior dovetails neatly with the assumptions of ASTM D5229, which was employed to extract both the diffusion coefficient (Dz) and the final equilibrium moisture content ($M\infty$) [50].

By the time the test finished the neat epoxy (NE) showed the gain about +0.19 g. The wood-graphene composites (WG) took up a bit more landing in the +0.21 to +0.25 g range. In contrast the densified wood-graphene composites (DW) swelled the most, spanning +0.26,

to +0.38 g. Expressed as a percentage of the weight (Day 0) NE's uptake was roughly 1.7 % WG's lay between 2.65 % and 2.78 % and DW absorbed the greatest amount ranging from about 3.49 % to 5.37 %. Overall, the densified wood composites clearly took up more moisture compared to the normal wood group.

Since epoxy absorbs much less water than wood (because it has fewer –OH groups that attract moisture), the neat epoxy sample showed the lowest weight gain and reached its saturation point earlier than the wood-based composites [71], [72]. For WG and DW samples, although densified wood (DW) is more compact, it absorbed more water in this study. Densification can reduce moisture uptake by limiting accessible –OH sites. In densified wood the cell walls are less porous compared to normal wood in this experiment is found in SEM. Diffusivity depends on the cell wall structure and porosity. Densification compresses the wood structure by collapsing or narrowing cell lumens, intercellular voids, and microchannels. This reduces the connectivity and size of pathways for moisture diffusion [73]. So, the densified wood samples show lower diffusivity.

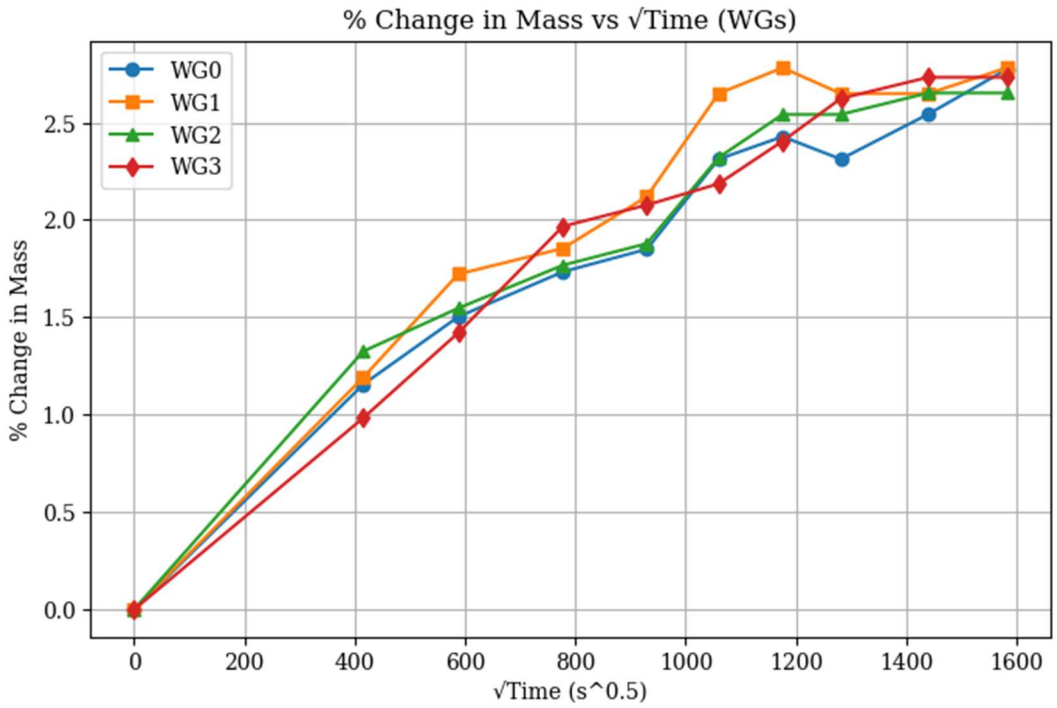

Figure 25: Change in mass vs √time of WG samples

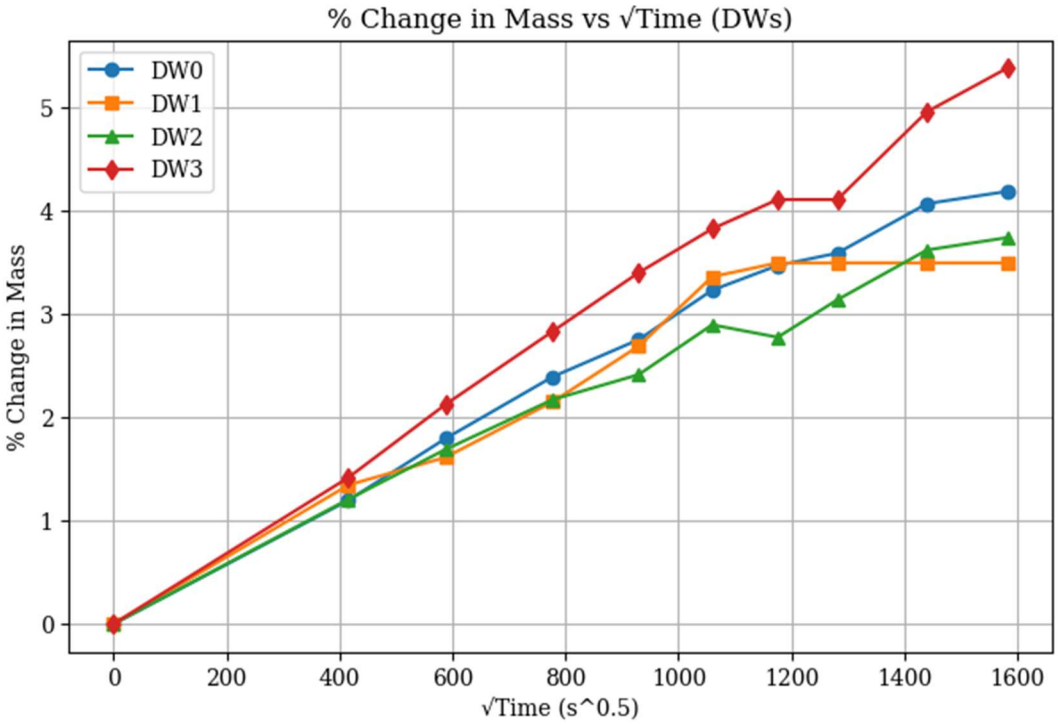

Figure 26: Change in mass vs √time of WG samples

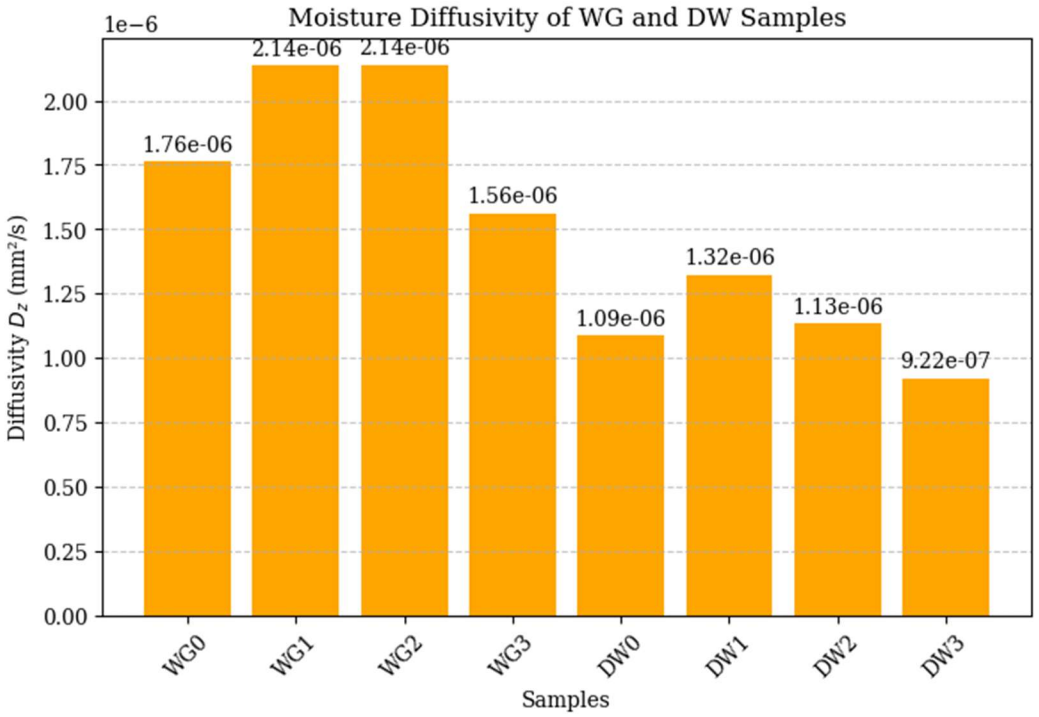

Figure 27: Comparison of moisture diffusivity between WG and DW samples at varying graphene content (0%, 0.1%, 0.2%, 0.3% wt)

This explains the behavior of the DW samples in this study that, the compression process decreased the internal surface area by crushing some cell walls and the microcracks are filled by epoxy. As a result, although densified wood can absorb more water than normal wood during immersion, but the diffusivity is less than the normal wood.

Graphene particles in epoxy can slow moisture absorption by forcing water to take a longer path around the particles that effectively reduces diffusivity and permeability. This barrier effect works best when the particles are well-dispersed, aligned, and have a high aspect ratio [74]. In densified wood, graphene particles are well dispersed that reduced the diffusivity in each set of samples containing different amount of graphene in both normal and densified wood.

4.7. TGA and DSC

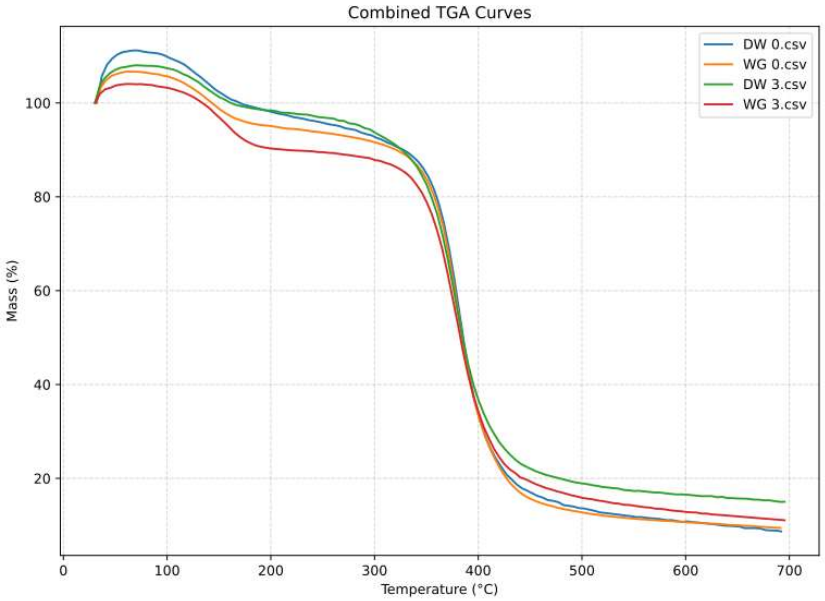

Figure 28: Combined TGA curves

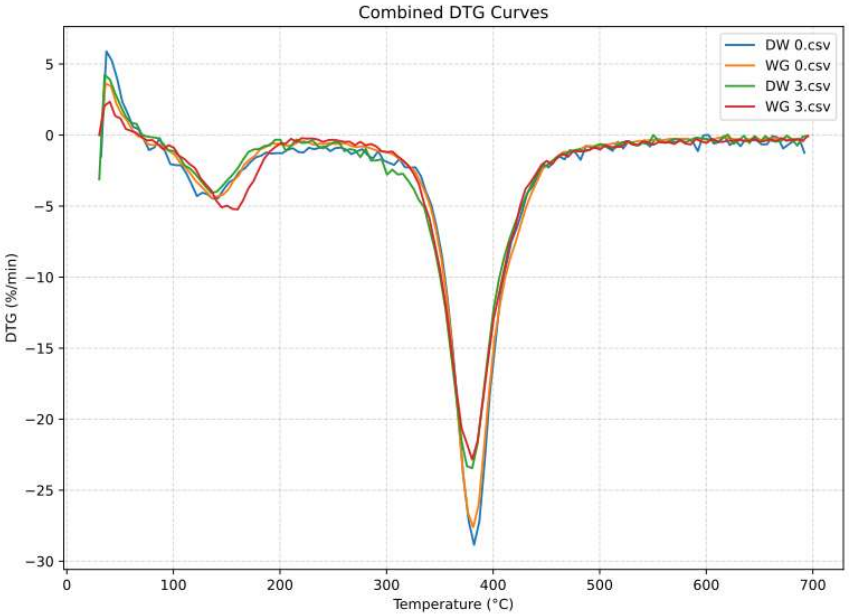

Figure 29: Combined DTG curves

Table 4: DTG values

Sample	Start of decomposition, ºC	5% Weight Loss, ºC	10% Weight Loss, ºC	50% Weight Loss, ºC	Residual Sample Weight at 600 ºC
DW 0	116	267	327	385	10.80
WG 0	105	202	320	384	10.66
DW 3	115	287	326	384	16.54
WG 3	122	159	215	383	12.86

TGA graphs were carried out for two extreme ends of our investigational sample groups. For densified wood composite, DW 0 and DW 3 and for normal wood flour WG 0 and WG 3. The decomposition trend of the samples showed a good deal of variety with DW 0 starting at 116 ºC while WG 0 at 105 ºC. For 5% weight loss, DW 0 samples performed better than WG 0 samples by reaching 50 ºC more than WG 0 for the same levels of decomposition. However, this difference is not maintained for long as both DW 0 and WG 0 samples go through 10% weight loss at 327 and 320 ºC. This delay in initial decomposition of the DW 0 samples over the WG 0 samples can be traced to the highly compact structure of the densified wood fiber which restricts the flow of oxygen through the channels [75]. Moreover, the higher crystallinity of the densified wood fiber might have pushed the decomposition temperature to the higher regions [76]. To add to the point, alkaline treatments are known to improve the thermal stability at initial temperatures due to fibrillation effect which influences better mechanical interlocking [77], [78].

For 0.3% added samples, DW 3 outperformed WG 3 similarly in terms of thermal stability in all the stages of heating with 16% residual left at the end of the process [75], [76], [77], [78]. The 0.3% graphene addition might provide percolative paths for electrons to move through inside the DW 3 samples resulting in better thermal conductivity and lesser decomposition [79]. However, a contrasting image can be seen for WG 3 which shows the minimal stability of the four samples for

the first half loss of mass. While GNP impregnates densified wood microstructure easily, the rougher hydrophilic surface and voids promote agglomeration which restricts thermal stability [80], [81] . The DTG curves also show the same phenomenon where the DW 0 and DW 3 dips are at a slightly higher temperature to the right than WG 0 and WG 3 respectively proving slower decomposition.

Lower char formation of DW samples at the end of the application of heat up to 600 ºC can also be attributed to the alkali treatment of the densified wood [77], [78]. The lower mass loss rate of the DW samples till the end can be attributed to the increased thermal inertia due to the higher density packing of the densified wood fiber [82].

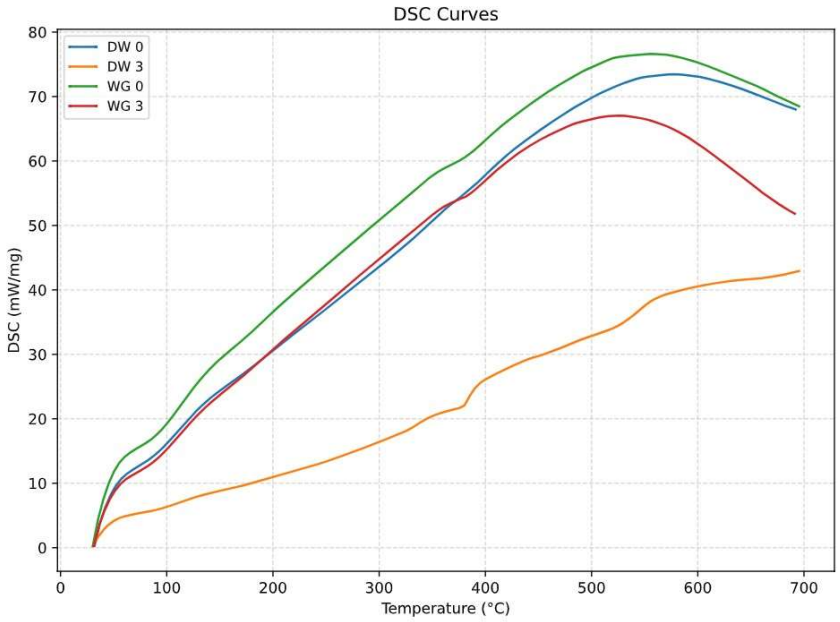

Figure 30: DSC curves at varying graphene content (0%, 0.1%, 0.2%, 0.3% wt)

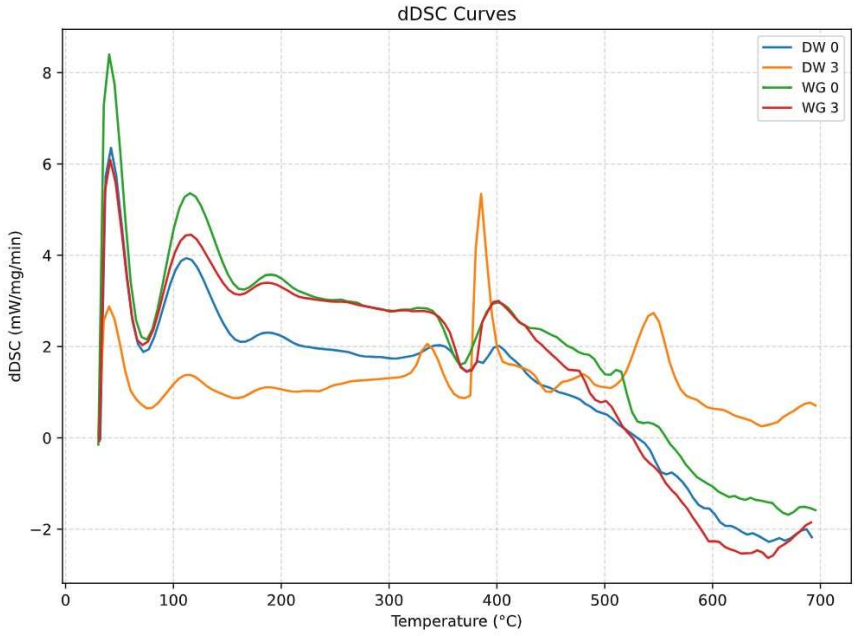

Figure 31: dDSC curves at varying graphene content (0%, 0.1%, 0.2%, 0.3% wt)

The DSC curves show that WG 0 and WG 3 are more thermally active at initial temperatures which indicate the faster decomposition of these samples at slightly lower temperatures compared to DW 0 and DW 3 from the TGA plots [75], [76]. The lower baseline for DW 3 in the DSC graph represents lower energetic decomposition like the ones as seen in the TGA plots. For addition of 0.3% graphene, both DW 3 and WG 3 shows suppressed heat flow compared to DW 0 and WG 0 respectively. However, the DSC curve of WG 3 follows the WG 0 curve very closely compared to the large difference between DW 3 and DW 0. Such contrasting difference after adding graphene, between the WG ones and the DW ones can be attributed to better percolation channels created in the DW samples which is evident from the TGA results [79], [81]. The dDSC curves confirm that graphene reduces the decomposition and enthalpy change without delaying the temperature promoting further stability and higher char yield [79].

4.8. Comparison and Potential Applications

A comparative analysis between densified (DW) and normal (WG) wood/epoxy/graphene composites clearly highlights the effectiveness of densification in enhancing overall performance. In every test category mechanical, thermal, electrical and diffusivity, the DW composites outperformed the WG counterparts. Densification compressed the wood cell walls, reduced porosity and improved epoxy infiltration which strengthened filler matrix adhesion and stress transfer. The tensile and flexural strengths of the DW composites jumped by 15–40 % compared with the WG samples and the impact strength peaked at a content of 0.2 wt %, to more effective crack deflection and energy absorption. Thermal testing revealed that DW specimens decompose at temperatures and retain residual char underscoring their superior thermal stability. Moreover the tighter fiber packing in the DW composites encourages the formation of conductive networks resulting in higher electrical conductivity at the same graphene loading. Although DW composites took up a touch moisture overall their diffusivity stayed lower due, to the connectivity of their internal pores.

The synergistic blend of densified wood flour and graphene nanoplatelets makes these hybrid composites a standout option, for a range of engineering uses. Their striking strength-to-weight ratio, with toughness and thermal resilience suits them for structural panels, building insulators, automotive interior trims, electronic casings and lightweight furniture components [83]. Moreover the boost of the electrical conductivity opens doors to coatings, electromagnetic shielding materials and smart bio-composite systems [84]. By opting for fillers and keeping the graphene content low these composites not only stick to sustainable material design principles but also carve out an eco-efficient path, toward the next generation of high-performance polymer composites.

Chapter 5: Conclusion and Future Recommendation

This investigation took a dive into how densifying wood reshapes the thermal, electrical and diffusivity behavior of wood/epoxy/graphene nanocomposites. The results make it unmistakably clear that densified wood flour (DW) pulls ahead of wood flour (WG) thanks, to a tighter-packed microstructure an orderly fiber arrangement and a sturdier interfacial grip, on the epoxy matrix.

Embedding the nanoparticles (GNP) to the material gave the composites a boost of reinforcement. The sweet spot appeared at a 0.2 wt % loading. At that concentration the graphene spread uniformly by allowing stress to travel efficient way and by triggering crack deflection and bridging mechanisms that together lifted tensile strength, modulus and impact resistance. Adding graphene beyond this point led to agglomeration, which in turn sapped the performance.

The TGA/DSC data point to a shift, toward decomposition onset temperatures and an increase in char in the densified composites underscoring a boost, in thermal stability. Graphene's inclusion spiked the conductivity dramatically in the DW specimens, where the fibers are squeezed tighter together and forge a more robust conductive lattice. Even though the densified wood swallows up moisture in total its moisture diffusivity drops, a result of the interpore connectivity.

In summary, the synergistic combination of densified wood flour and graphene produced bio based composites with superior strength, toughness, and thermal resistance. These findings establish densification as an effective strategy to optimize natural fillers for high performance, sustainable polymer composites suitable for semi-structural, insulating and functional applications.

Future recommendation for this work-

- The study can be extended by optimizing graphene dispersion methods and exploring different densification parameters to further enhance the mechanical and thermal performance of the composites.

- Future work may focus on using bio-based or recyclable epoxy matrices and advanced surface modification of wood flour to develop a fully sustainable composite system.

- Long-term durability, ageing behavior and large-scale manufacturing feasibility should be investigated to evaluate industrial applications in structural, electrical and insulation components.

References:

[1] L. Li *et al.*, "Sustainable engineering polymer composites fabricated using delignified bamboo fiber as reinforcement and walnut shell powder as filler," *Compos B Eng*, vol. 287, p. 111857, Dec. 2024, doi: 10.1016/j.compositesb.2024.111857.

[2] S. K. Jakab, V. L. Bódi, and L. Lendvai, "The Effect of Wood Flour Incorporation on the Properties of Injection Molded Poly(Lactic Acid) Products," in *SMTS 2024*, Basel Switzerland: MDPI, Nov. 2024, p. 43. doi: 10.3390/engproc2024079043.

[3] Z. Mitaľová, D. Mitaľ, and K. Berladir, "A Concise Review of the Components and Properties of Wood–Plastic Composites," *Polymers (Basel)*, vol. 16, no. 11, p. 1556, May 2024, doi: 10.3390/polym16111556.

[4] W. Yu, R. Qiu, W. Lei, and Y. Chen, "Effects of Modification on Properties of Wood Flour/PBAT Biocomposites," *Polymers (Basel)*, vol. 17, no. 5, p. 555, Feb. 2025, doi: 10.3390/polym17050555.

[5] P. Mania, C. Kupfernagel, and S. Curling, "Densification of Delignified Wood: Influence of Chemical Composition on Wood Density, Compressive Strength, and Hardness of Eurasian Aspen and Scots Pine," *Forests*, vol. 15, no. 6, p. 892, May 2024, doi: 10.3390/f15060892.

[6] J. Song *et al.*, "Processing bulk natural wood into a high-performance structural material," *Nature*, vol. 554, no. 7691, pp. 224–228, Feb. 2018, doi: 10.1038/nature25476.

[7] S. Wilczewski, Z. Nowak, M. Maj, M. Osial, R. Minikayev, and M. Giersig, "Enhancing Epoxy Composites with Graphene and Graphene Oxide: Thermal and Mechanical Insights," *ChemNanoMat*, vol. 11, no. 2, Feb. 2025, doi: 10.1002/cnma.202400488.

[8] W. Zhu *et al.*, "The functional graphene/epoxy resin composites prepared by novel two-phase extraction towards enhancing mechanical properties and thermal stability," *Front Chem*, vol. 12, 2024, doi: 10.3389/fchem.2024.1433727.

[9] G. Verma, R. Goel, N. Kaur, M. K. Singh, S. M. Rangappa, and S. Siengchin, "Understanding behaviour of graphene in natural fibre composites: A comprehensive review," *Eur Polym J*, vol. 232, p. 113959, May 2025, doi: 10.1016/j.eurpolymj.2025.113959.

[10] Z. He *et al.*, "Enhancing the electromagnetic interference shielding of epoxy resin composites with hierarchically structured MXene/graphene aerogel," *Compos B Eng*, vol. 274, p. 111230, Apr. 2024, doi: 10.1016/j.compositesb.2024.111230.

[11] M. Bahrami, J. Abenojar, and M. Á. Martínez, “Recent Progress in Hybrid Biocomposites: Mechanical Properties, Water Absorption, and Flame Retardancy,” *Materials*, vol. 13, no. 22, p. 5145, Nov. 2020, doi: 10.3390/ma13225145.

[12] M. R. Ahmed, L. Maio, and P. Potluri, “Graphene-enhanced epoxy composites: A comprehensive review of dispersion mechanisms, processing strategies, property optimization, characterization and sustainable innovations,” *Progress in Aerospace Sciences*, vol. 158, p. 101142, Oct. 2025, doi: 10.1016/j.paerosci.2025.101142.

[13] S. Saito, S. Sato, and Y. Arao, “The effect of processing/curing temperature and viscosity of epoxy resins on the flexural/tensile properties of GNP-epoxy resin nanocomposites,” *Compos Part A Appl Sci Manuf*, vol. 183, p. 108222, Aug. 2024, doi: 10.1016/j.compositesa.2024.108222.

[14] G. Pokhrel, Y. Han, and D. J. Gardner, “Comparative Study of the Properties of Wood Flour and Wood Pellets Manufactured from Secondary Processing Mill Residues,” *Polymers (Basel)*, vol. 13, no. 15, p. 2487, Jul. 2021, doi: 10.3390/polym13152487.

[15] K. M. F. Hasan *et al.*, “Sustainable prospects of lignocellulosic wood and natural fiber-based materials in 3D and 4D printing,” *Adv Compos Hybrid Mater*, vol. 8, no. 2, p. 189, Apr. 2025, doi: 10.1007/s42114-025-01273-6.

[16] Md. Saiful Islam, S. Hamdan, I. Jusoh, Md. Rezaur Rahman, and A. S. Ahmed, “The effect of alkali pretreatment on mechanical and morphological properties of tropical wood polymer composites,” *Mater Des*, vol. 33, pp. 419–424, Jan. 2012, doi: 10.1016/j.matdes.2011.04.044.

[17] A. Sienkiewicz and P. Czub, “Functional Management of Waste Wood Flour as an Example of a ‘Greener’ Approach towards the Synthesis of Bio-Based Epoxy Resins,” *Polymers (Basel)*, vol. 15, no. 17, p. 3521, Aug. 2023, doi: 10.3390/polym15173521.

[18] M. Z. R. Khan, S. K. Srivastava, and M. K. Gupta, “A state-of-the-art review on particulate wood polymer composites: Processing, properties and applications,” *Polym Test*, vol. 89, p. 106721, Sep. 2020, doi: 10.1016/j.polymertesting.2020.106721.

[19] A. H. Elsheikh, H. Panchal, S. Shanmugan, T. Muthuramalingam, Ahmed. M. El-Kassas, and B. Ramesh, “Recent progresses in wood-plastic composites: Pre-processing treatments, manufacturing techniques, recyclability and eco-friendly assessment,” *Clean Eng Technol*, vol. 8, p. 100450, Jun. 2022, doi: 10.1016/j.clet.2022.100450.

[20] B. C. Bal, “Mechanical properties of wood-plastic composites produced with recycled polyethylene, used Tetra Pak® boxes, and wood flour,” *Bioresources*, vol. 17, no. 4, pp. 6569–6577, Oct. 2022, doi: 10.15376/biores.17.4.6569-6577.

[21] K. K. Khoaele, O. J. Gbadeyan, V. Chunilall, and B. Sithole, “A review on waste wood reinforced polymer composites and their processing for construction materials,” *International Journal of Sustainable Engineering*, vol. 16, no. 1, pp. 104–116, Dec. 2023, doi: 10.1080/19397038.2023.2214162.

[22] D. Basalp, F. Tihminlioglu, S. C. Sofuoglu, F. Inal, and A. Sofuoglu, “Utilization of Municipal Plastic and Wood Waste in Industrial Manufacturing of Wood Plastic Composites,” *Waste Biomass Valorization*, vol. 11, no. 10, pp. 5419–5430, Oct. 2020, doi: 10.1007/s12649-020-00986-7.

[23] W. K. Chee, H. N. Lim, N. M. Huang, and I. Harrison, “Nanocomposites of graphene/polymers: a review,” *RSC Adv*, vol. 5, no. 83, pp. 68014–68051, Aug. 2015, doi: 10.1039/C5RA07989F.

[24] S. J. Lee, S. J. Yoon, and I.-Y. Jeon, “Graphene/Polymer Nanocomposites: Preparation, Mechanical Properties, and Application,” *Polymers (Basel)*, vol. 14, no. 21, p. 4733, Nov. 2022, doi: 10.3390/polym14214733.

[25] A. Liang, X. Jiang, X. Hong, Y. Jiang, Z. Shao, and D. Zhu, “Recent Developments Concerning the Dispersion Methods and Mechanisms of Graphene,” *Coatings*, vol. 8, no. 1, p. 33, Jan. 2018, doi: 10.3390/coatings8010033.

[26] S. Perumal, R. Atchudan, and I. W. Cheong, “Recent Studies on Dispersion of Graphene–Polymer Composites,” *Polymers (Basel)*, vol. 13, no. 14, p. 2375, Jul. 2021, doi: 10.3390/polym13142375.

[27] A. Olean-Oliveira, G. A. Oliveira Brito, C. X. Cardoso, and M. F. S. Teixeira, “Nanocomposite Materials Based on Electrochemically Synthesized Graphene Polymers: Molecular Architecture Strategies for Sensor Applications,” *Chemosensors*, vol. 9, no. 6, p. 149, Jun. 2021, doi: 10.3390/chemosensors9060149.

[28] A. Kiziltas, W. Liu, S. Tamrakar, and D. Mielewski, “Graphene nanoplatelet reinforcement for thermal and mechanical properties enhancement of bio-based polyamide 6, 10 nanocomposites for automotive applications,” *Composites Part C: Open Access*, vol. 6, p. 100177, Oct. 2021, doi: 10.1016/j.jcomc.2021.100177.

[29] Y.-C. Chiou, H.-Y. Chou, and M.-Y. Shen, “Effects of adding graphene nanoplatelets and nanocarbon aerogels to epoxy resins and their carbon fiber composites,” *Mater Des*, vol. 178, p. 107869, Sep. 2019, doi: 10.1016/j.matdes.2019.107869.

[30] F. da Luz, F. Garcia Filho, M. del-Río, L. Nascimento, W. Pinheiro, and S. Monteiro, “Graphene-Incorporated Natural Fiber Polymer Composites: A First Overview,” *Polymers (Basel)*, vol. 12, no. 7, p. 1601, Jul. 2020, doi: 10.3390/polym12071601.

[31] D. Niyobuhungiro and L. Hong, “Graphene Polymer Composites: Review on Fabrication Method, Properties and Future Perspectives,” *Advances in Science and Technology Research Journal*, vol. 15, no. 1, pp. 37–49, Mar. 2021, doi: 10.12913/22998624/129680.

[32] A. Gholizadeh, A. Babaei, and M. Haji Abdolrasouli, “Effect of functionalized graphene on mechanical and rheological properties of melt processed polyamide 6 nanocomposites,” *Polym Compos*, vol. 46, no. 7, pp. 6696–6713, May 2025, doi: 10.1002/pc.29389.

[33] H. Yang, Z. Deng, M. Shi, and Z. Huang, “High-Thermal-Conductivity Graphene/Epoxy Resin Composites: A Review of Reinforcement Mechanisms, Structural Regulation and Application Challenges,” *Polymers (Basel)*, vol. 17, no. 17, p. 2342, Aug. 2025, doi: 10.3390/polym17172342.

[34] M. Fuseini, M. M. Yousry Zaghloul, D. Abakar, and M. M. Yousry Zaghloul, “Review of epoxy nano-filled hybrid nanocomposite coatings for tribological applications,” *FlatChem*, vol. 49, p. 100768, Jan. 2025, doi: 10.1016/j.flatc.2024.100768.

[35] P. Mohan, “A Critical Review: The Modification, Properties, and Applications of Epoxy Resins,” *Polym Plast Technol Eng*, vol. 52, no. 2, pp. 107–125, Jan. 2013, doi: 10.1080/03602559.2012.727057.

[36] “LAPOX ® METALAM-B,” 2017, Accessed: Oct. 12, 2025. [Online]. Available: www.atul.co.in

[37] R. Dallaev, T. Pisarenko, N. Papež, P. Sadovský, and V. Holcman, “A Brief Overview on Epoxies in Electronics: Properties, Applications, and Modifications,” *Polymers (Basel)*, vol. 15, no. 19, p. 3964, Sep. 2023, doi: 10.3390/polym15193964.

[38] J. Huang, P. Fu, W. Li, L. Xiao, J. Chen, and X. Nie, “Influence of crosslinking density on the mechanical and thermal properties of plant oil-based epoxy resin,” *RSC Adv*, vol. 12, no. 36, pp. 23048–23056, 2022, doi: 10.1039/D2RA04206A.

[39] M.-H. Zhou, G.-Z. Yin, and S. González Prolongo, “Review of thermal conductivity in epoxy thermosets and composites: Mechanisms, parameters, and filler influences,” *Advanced Industrial and Engineering Polymer Research*, vol. 7, no. 3, pp. 295–308, Jul. 2024, doi: 10.1016/j.aiepr.2023.08.003.

[40] D. Matykiewicz, “Hybrid Epoxy Composites with Both Powder and Fiber Filler: A Review of Mechanical and Thermomechanical Properties,” *Materials*, vol. 13, no. 8, p. 1802, Apr. 2020, doi: 10.3390/ma13081802.

[41] J. J. Fekiač *et al.*, “Comprehensive Review: Optimization of Epoxy Composites, Mechanical Properties, & Technological Trends,” *Polymers (Basel)*, vol. 17, no. 3, p. 271, Jan. 2025, doi: 10.3390/polym17030271.

[42] W. Huang, Y. Jin, Y. Guo, J. Deng, H. Yu, and B. He, “Fabrication of High-Performance Densified Wood via High-Pressure Steam Treatment and Hot-Pressing,” *Polymers (Basel)*, vol. 16, no. 7, p. 939, Mar. 2024, doi: 10.3390/polym16070939.

[43] “Mesh Sizing Chart for strainers.” Accessed: Oct. 09, 2025. [Online]. Available: https://www.valvesonline.com.au/references/mesh-sizing-chart/?srsltid=AfmBOooAb-YROFinUjrwEPZmy4eADULHYd29iEv2zK0IsGm2sgR4nXu3

[44] M. P. B H *et al.*, “Effect of Teak Wood Dust as Filler Material on Mechanical Properties of Abaca-Pineapple-Epoxy Hybrid Composite,” *Journal of Natural Fibers*, vol. 21, no. 1, Dec. 2024, doi: 10.1080/15440478.2024.2434603.

[45] R. Yu, P. M.N., J. Feng, Y. Yang, S. H. Hong, and J. Song, “Enhancing the mechanical properties of flax fiber-reinforced epoxy composites through cellulose nanofiber incorporation,” *Ind Crops Prod*, vol. 223, p. 120113, Jan. 2025, doi: 10.1016/j.indcrop.2024.120113.

[46] V. C. Dinkar and V. Kumar, “A review study on the mechanical behaviour of natural fibre-reinforced epoxy composite,” *Polymer Bulletin*, vol. 82, no. 15, pp. 9647–9682, Oct. 2025, doi: 10.1007/s00289-025-05902-4.

[47] “Highly efficient single-step pretreatment to remove lignin and hemicellulose from softwood :: BioResources.” Accessed: Oct. 09, 2025. [Online]. Available: https://bioresources.cnr.ncsu.edu/resources/highly-efficient-single-step-pretreatment-to-remove-lignin-and-hemicellulose-from-softwood/?

[48] L.-C. Tang *et al.*, “The effect of graphene dispersion on the mechanical properties of graphene/epoxy composites,” *Carbon N Y*, vol. 60, pp. 16–27, Aug. 2013, doi: 10.1016/j.carbon.2013.03.050.

[49] “ASTM D638: tensile properties plastics | ZwickRoell.” Accessed: Oct. 09, 2025. [Online]. Available: https://www.zwickroell.com/industries/plastics/thermoplastics-and-thermosetting-molding-materials/tensile-properties-astm-d638/

[50] A. International and files indexed by mero, “Standard Test Method for Moisture Absorption Properties and Equilibrium Conditioning of Polymer Matrix Composite Materials 1.” [Online]. Available: www.astm.org,

[51] “D4812 Standard Test Method for Unnotched Cantilever Beam Impact Resistance of Plastics.” Accessed: Oct. 09, 2025. [Online]. Available: https://store.astm.org/d4812-19e01.html

[52] “Test Methods for Flexural Properties of Unreinforced and Reinforced Plastics and Electrical Insulating Materials,” Jul. 2017, doi: 10.1520/D0790-17.

[53] “E1131 Standard Test Method for Compositional Analysis by Thermogravimetry.” Accessed: Oct. 10, 2025. [Online]. Available: https://store.astm.org/e1131-20.html

[54] “D3418 Standard Test Method for Transition Temperatures and Enthalpies of Fusion and Crystallization of Polymers by Differential Scanning Calorimetry.” Accessed: Oct. 10, 2025. [Online]. Available: https://store.astm.org/d3418-15.html

[55] A. Paydayesh, F. Pashaei Soorbaghi, A. Aref Azar, and A. Jalali-Arani, “Electrical conductivity of graphene filled PLA/PMMA blends: Experimental investigation and modeling,” *Polym Compos*, vol. 40, no. 2, pp. 704–715, Feb. 2019, doi: 10.1002/pc.24722.

[56] “Test Methods for DC Resistance or Conductance of Insulating Materials,” May 15, 2007, *ASTM International, West Conshohocken, PA*. doi: 10.1520/D0257-07.

[57] M. Akter, H. Ozdemir, and K. Bilisik, “Epoxy/Graphene Nanoplatelet (GNP) Nanocomposites: An Experimental Study on Tensile, Compressive, and Thermal Properties,” *Polymers (Basel)*, vol. 16, no. 11, p. 1483, May 2024, doi: 10.3390/polym16111483.

[58] J. Keyte, K. Pancholi, and J. Njuguna, “Recent Developments in Graphene Oxide/Epoxy Carbon Fiber-Reinforced Composites,” *Front Mater*, vol. 6, Oct. 2019, doi: 10.3389/fmats.2019.00224.

[59] W. Huang, Y. Jin, Y. Guo, J. Deng, H. Yu, and B. He, “Fabrication of High-Performance Densified Wood via High-Pressure Steam Treatment and Hot-Pressing,” *Polymers (Basel)*, vol. 16, no. 7, p. 939, Mar. 2024, doi: 10.3390/polym16070939.

[60] M. Jakob, G. Stemmer, I. Czabany, U. Müller, and W. Gindl-Altmutter, “Preparation of High Strength Plywood from Partially Delignified Densified Wood,” *Polymers (Basel)*, vol. 12, no. 8, p. 1796, Aug. 2020, doi: 10.3390/polym12081796.

[61] D. Novel *et al.*, “Strengthening of Wood-like Materials via Densification and Nanoparticle Intercalation,” *Nanomaterials*, vol. 10, no. 3, p. 478, Mar. 2020, doi: 10.3390/nano10030478.

[62] X. Huang, D. Yang, and Z. Kang, “Impact of pore distribution characteristics on percolation threshold based on site percolation theory,” *Physica A: Statistical Mechanics and its Applications*, vol. 570, p. 125800, May 2021, doi: 10.1016/j.physa.2021.125800.

[63] D. Guo, S. Yang, F. Fu, G. Li, and F. Chu, “New strategy for the preparation of ultra-high-strength wood-epoxy polymer composites,” *Composites Communications*, vol. 33, p. 101191, Aug. 2022, doi: 10.1016/j.coco.2022.101191.

[64] J. P. Cabral, B. Kafle, M. Subhani, J. Reiner, and M. Ashraf, “Densification of timber: a review on the process, material properties, and application,” *Journal of Wood Science*, vol. 68, no. 1, pp. 1–24, Dec. 2022, doi: 10.1186/S10086-022-02028-3/FIGURES/13.

[65] J. M. Parente, R. Simões, and P. N. B. Reis, “Effect of graphene nanoparticles on suspension viscosity and mechanical properties of epoxy-based nanocomposites,” *Procedia Structural Integrity*, vol. 37, pp. 820–825, 2022, doi: 10.1016/j.prostr.2022.02.014.

[66] Y. Wang *et al.*, “Study on Graphene-Reinforced Epoxy Solvent-Borne High-Temperature-Resistant Adhesives for Bonding C/C Composites Under Extreme Temperatures,” *Materials*, vol. 18, no. 17, p. 4213, Sep. 2025, doi: 10.3390/ma18174213.

[67] S. Stankovich *et al.*, “Graphene-based composite materials,” *Nature*, vol. 442, no. 7100, pp. 282–286, Jul. 2006, doi: 10.1038/nature04969.

[68] T. Kuilla, S. Bhadra, D. Yao, N. H. Kim, S. Bose, and J. H. Lee, “Recent advances in graphene based polymer composites,” *Prog Polym Sci*, vol. 35, no. 11, pp. 1350–1375, Nov. 2010, doi: 10.1016/j.progpolymsci.2010.07.005.

[69] G. Chen *et al.*, “A Highly Conductive Cationic Wood Membrane,” *Adv Funct Mater*, vol. 29, no. 44, Nov. 2019, doi: 10.1002/adfm.201902772.

[70] X. Ma *et al.*, “Ultrathin Wood-Derived Conductive Carbon Composite Film for Electromagnetic Shielding and Electric Heating Management,” *Adv Funct Mater*, vol. 33, no. 16, Apr. 2023, doi: 10.1002/adfm.202213431.

[71] Y. Ratna Pratiwi, I. Widiastuti, and B. Harjanto, “Studies on Water Sorption Behaviour of Laminated Bamboo Polymer Composite,” *E3S Web of Conferences*, vol. 130, p. 01040, Nov. 2019, doi: 10.1051/e3sconf/201913001040.

[72] A. Ashori and A. Kuzmin, “Effect of chitosan-epoxy ratio in bio-based adhesive on physical and mechanical properties of medium density fiberboards from mixed hardwood fibers,” *Sci Rep*, vol. 14, no. 1, p. 5057, Mar. 2024, doi: 10.1038/s41598-024-55796-x.

[73] W. Kang, Y. H. Lee, W. Y. Chung, and H. L. Xu, “Parameter estimation of moisture diffusivity in wood by an inverse method,” *Journal of Wood Science*, vol. 55, no. 2, pp. 83–90, Apr. 2009, doi: 10.1007/S10086-008-1006-0/METRICS.

[74] A. Oun, A. Manalo, O. Alajarmeh, R. Abousnina, and A. Gerdes, “Long-Term Water Absorption of Hybrid Flax Fibre-Reinforced Epoxy Composites with Graphene and Its Influence on Mechanical Properties,” *Polymers (Basel)*, vol. 14, no. 17, p. 3679, Sep. 2022, doi: 10.3390/polym14173679.

[75] W. Gan *et al.*, “Dense, Self-Formed Char Layer Enables a Fire-Retardant Wood Structural Material,” *Adv Funct Mater*, vol. 29, no. 14, Apr. 2019, doi: 10.1002/adfm.201807444.

[76] U.-J. Kim, S. H. Eom, and M. Wada, “Thermal decomposition of native cellulose: Influence on crystallite size,” *Polym Degrad Stab*, vol. 95, no. 5, pp. 778–781, May 2010, doi: 10.1016/j.polymdegradstab.2010.02.009.

[77] N. M. Nurazzi *et al.*, “Thermogravimetric Analysis Properties of Cellulosic Natural Fiber Polymer Composites: A Review on Influence of Chemical Treatments,” *Polymers (Basel)*, vol. 13, no. 16, p. 2710, Aug. 2021, doi: 10.3390/polym13162710.

[78] B. S. Yew, M. Muhamad, S. B. Mohamed, and F. H. Wee, “Effect of Alkaline Treatment on Structural Characterisation, Thermal Degradation and Water Absorption Ability of Coir Fibre Polymer Composites,” *Sains Malays*, vol. 48, no. 3, pp. 653–659, Mar. 2019, doi: 10.17576/jsm-2019-4803-19.

[79] M. Akter, H. Ozdemir, and K. Bilisik, “Epoxy/Graphene Nanoplatelet (GNP) Nanocomposites: An Experimental Study on Tensile, Compressive, and Thermal Properties,” *Polymers (Basel)*, vol. 16, no. 11, p. 1483, May 2024, doi: 10.3390/polym16111483.

[80] F. Xie, S. H. Qi, and D. Wu, “A facile strategy for the reduction of graphene oxide and its effect on thermal conductivity of epoxy based composites,” *Express Polym Lett*, vol. 10, no. 6, pp. 470–478, 2016, doi: 10.3144/expresspolymlett.2016.45.

[81] J. Wei, T. Vo, and F. Inam, “Epoxy/graphene nanocomposites – processing and properties: a review,” *RSC Adv*, vol. 5, no. 90, pp. 73510–73524, 2015, doi: 10.1039/C5RA13897C.

[82] Y. Zhou *et al.*, “Influences of Species and Density on the Horizontal Flame Spread Behavior of Densified Wood,” *Buildings*, vol. 14, no. 3, p. 620, Feb. 2024, doi: 10.3390/buildings14030620.

[83] Y.-F. Shih, C.-W. Chang, T.-H. Hsu, and W.-Y. Dai, “Application of Sustainable Wood-Plastic Composites in Energy-Efficient Construction,” *Buildings*, vol. 14, no. 4, p. 958, Apr. 2024, doi: 10.3390/buildings14040958.

[84] K. Tserpes, V. Tzatzadakis, and J. Bachmann, “Electrical Conductivity and Electromagnetic Shielding Effectiveness of Bio-Composites,” *Journal of Composites Science*, vol. 4, no. 1, p. 28, Mar. 2020, doi: 10.3390/jcs4010028.